UPPSALA
UNIVERSITET

Digital Comprehensive Summaries of Uppsala Dissertations from the Faculty of Pharmacy 272

Proteomic and Functional Analysis of *In Vitro* Systems for Studies of Drug Disposition in the Human Small Intestine and Liver

MAGNUS ÖLANDER

ACTA
UNIVERSITATIS
UPSALIENSIS
UPPSALA
2019

ISSN 1651-6192
ISBN 978-91-513-0668-1
urn:nbn:se:uu:diva-382406

Dissertation presented at Uppsala University to be publicly examined in Room B41, Biomedical center, Husargatan 3, Uppsala, Friday, 14 June 2019 at 09:15 for the degree of Doctor of Philosophy (Faculty of Pharmacy). The examination will be conducted in English. Faculty examiner: Associate Professor Volker Lauschke (Department of Physiology and Pharmacology, Karolinska Institutet).

Abstract
Ölander, M. 2019. Proteomic and Functional Analysis of *In Vitro* Systems for Studies of Drug Disposition in the Human Small Intestine and Liver. *Digital Comprehensive Summaries of Uppsala Dissertations from the Faculty of Pharmacy* 272. 59 pp. Uppsala: Acta Universitatis Upsaliensis. ISBN 978-91-513-0668-1.

To reach the bloodstream, an orally administered drug must be absorbed through the small intestine and avoid extensive clearance in the liver. Estimating these parameters *in vitro* is therefore important in drug discovery and development. This can be achieved with cellular models that simulate human organ function, such as Caco-2 cells and primary hepatocytes. No model fits every scenario, however, and this thesis aimed at using proteomic and functional analysis to better understand and increase the applicability of *in vitro* models based on Caco-2 cells and human hepatocytes.

First, the proteome of filter-grown Caco-2 cells was analyzed. This included near-complete coverage of enterocyte-related proteins, and over 300 ADME proteins. Further, by scaling uptake transport kinetics from Caco-2 cells to human jejunum, the importance of considering *in vitro--in vivo* expression differences to correctly interpret *in vitro* transport studies was demonstrated.

Focus was then turned to hepatocytes, where proteomics was used as a basis for the successful development of an apoptosis inhibition protocol for restoration of attachment properties and functionality in suboptimal batches of cryopreserved human hepatocytes. As a spin-off project, image-based quantification of cell debris was developed into a novel apoptosis detection method.

Next, the *in vivo* heterogeneity of human hepatocytes was explored in an *in vitro* setting, where it was observed that human hepatocyte batches contain a wide range of cell sizes. By separating the cells into different size fractions, it was found that hepatocyte size corresponds to the microarchitectural zone of origin in the liver. Size separation can thus be used to study zonated liver functions *in vitro*.

Finally, the proteomes of the major types of non-parenchymal liver cells were analyzed, i.e. liver sinusoidal endothelial cells, Kupffer cells, and hepatic stellate cells. The different cell types all had distinctly different proteomes, and the expression of certain important ADME proteins indicated that non-parenchymal cells participate in drug disposition.

In conclusion, this thesis has improved the phenotypic understanding and extended the applicability of Caco-2 cells and primary human hepatocytes, two of the most important *in vitro* models for studies of small intestinal and hepatic drug disposition.

Keywords: proteomics, drug disposition, ADMET, drug transport, drug metabolism, hepatotoxicity, small intestine, liver, caco-2, human hepatocytes, cryopreservation, apoptosis, liver zonation, non-parenchymal cells

Magnus Ölander, Department of Pharmacy, Box 580, Uppsala University, SE-75123 Uppsala, Sweden.

ISSN 1651-6192
ISBN 978-91-513-0668-1
urn:nbn:se:uu:diva-382406 (http://urn.kb.se/resolve?urn=urn:nbn:se:uu:diva-382406)

Life, uh, finds a way.
Dr. Ian Malcolm

List of Papers

This thesis is based on the following papers, which are referred to in the text by their Roman numerals.

I **Ölander, M.**, Wiśniewski, J.R., Matsson, P., Lundquist, P., Artursson, P. (2016). The proteome of filter-grown Caco-2 cells with a focus on proteins involved in drug disposition. *Journal of Pharmaceutical Sciences*, 105(2):817-827.

II **Ölander, M.**, Wiśniewski, J.R., Flörkemeier, I., Handin, N., Urdzik, J., Artursson, P. (2019). A simple approach for restoration of differentiation and function in cryopreserved human hepatocytes. *Archives of Toxicology*, 93:819-829.

III **Ölander, M.**, Handin, N., Artursson, P. (2019) Image-based quantification of cell debris as a measure of apoptosis. *Analytical Chemistry*, DOI: 10.1021/acs.analchem.9b01243.

IV **Ölander, M.**, Wegler, C., Treyer, A., Flörkemeier, I., Handin, N., Pedersen, J.M., Vildhede, A., Mateus, A., LeCluyse, E.L., Urdzik, J., Artursson, P. Hepatocyte size fractionation allows dissection of human liver zonation. *In manuscript*.

V **Ölander, M.**, Wiśniewski, J.R, Artursson, P. Proteomic analysis of major cell types in the human liver. *In manuscript*.

Contents

Abbreviations

ADMET	Absorption, distribution, metabolism, excretion, and toxicity
ABC	ATP-binding cassette
CV	Central vein
CYP	Cytochrome P450
DHE	Dihydroethidium
DILI	Drug-induced liver injury
DMEM	Dulbecco's modified Eagle's medium
DPBS	Dulbecco's phosphate-buffered saline
ECM	Extracellular matrix
ER	Endoplasmic reticulum
FBS	Fetal bovine serum
GLS2	Glutaminase 2
GLUL	Glutamine synthetase
GST	Glutathione S-transferase
HBSS	Hank's balanced salt solution
HMM	Hepatocyte maintenance medium
HPA	Human Protein Atlas
HSC	Hepatic stellate cells
KC	Kupffer cells
LC/MS-MS	Liquid chromatography-tandem mass spectrometry
LSEC	Liver sinusoidal endothelial cells
MDCK	Madin-Darby canine kidney cells
MED-FASP	Multi-enzyme digestion filter-aided sample preparation
MHC	Major histocompatibility complex
NPC	Non-parenchymal cells
PAMPA	Parallel artificial membrane permeability assay
PCA	Principal component analysis
PEST	Penicillin-streptomycin
PLS	Partial least squares
PRR	Pattern recognition receptor
RNA-seq	RNA sequencing
ROS	Reactive oxygen species
SLC	Solute carrier
SULT	Sulfotransferase
TPA	Total protein approach
UGT	UDP-glucuronosyltransferase

Introduction

Many factors are involved in determining the extent to which an orally administered drug can enter the systemic circulation and reach its intended target (Figure 1). The dosage form (e.g. a tablet) must first disintegrate, followed by dissolution of the drug compound. The dissolved drug must then be absorbed through the small intestinal epithelium, and avoid extensive clearance by metabolism and biliary excretion in the liver. Furthermore, its beneficial effects must outweigh any adverse effects caused by toxicity. The usefulness of a drug is thus not only governed by its efficacy, but also by its properties in terms of absorption, distribution, metabolism, excretion, and toxicity (ADMET).

In vitro cell models that simulate the *in vivo* function of human organs greatly facilitate studies of pharmacokinetics, pharmacology, and toxicology. The ability of a drug compound to cross the small intestinal epithelium can be estimated by measuring its flux across a layer of intestine-derived cells grown on a permeable surface. One of the most widely used models in this context is the human colon carcinoma cell line Caco-2, which acquires enterocyte-like properties when cultured on polycarbonate filter supports.[1] Hepatic drug disposition, on the other hand, is commonly studied *in vitro* using isolated primary hepatocytes. Hepatocytes can be used in many different configurations in 2D and 3D culture, with varying degrees of complexity, liver-like function, and throughput.[2]

No model fits the needs of every application, however, and all *in vitro* systems come with their own particular drawbacks and uncertainties. For instance, cultured Caco-2 cells retain features of their cancerous origin,[3] and primary hepatocytes tend to dedifferentiate over time in culture.[4-6] Further, hepatocytes do not divide in culture,[7] and the resulting reliance on cryopreservation to ensure hepatocyte availability introduces additional problems. Most experimental setups require the cells to form cell-cell and cell-matrix interactions, and cryopreserved hepatocyte batches show substantial variability in this regard.[8-11] Hepatocytes also show considerable differences in expression and function throughout the liver microarchitecture,[12] and it is unclear whether isolated cell batches retain a representative mixture of subpopulations. Apart from hepatocyte heterogeneity, the liver contains a plethora of different non-parenchymal cells (NPCs).[13] The influence of NPCs on liver function is not taken into account in hepatocyte monocultures, and such cells are therefore sometimes added to generate more *in vivo*-like models.[2]

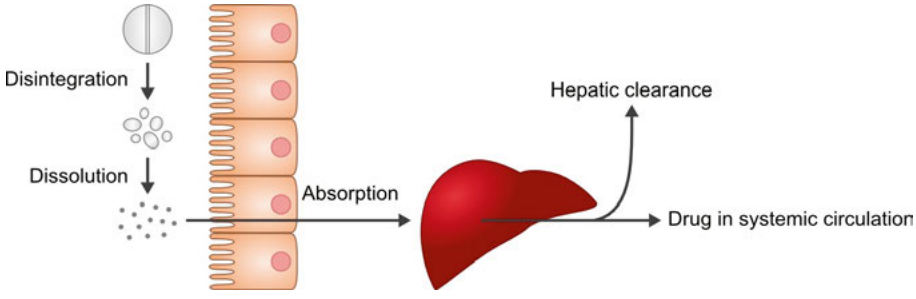

Figure 1. The sequence of events along the way to the systemic circulation for an orally administered drug. The amount of drug compound that reaches the circulation is highly dependent on the extent of absorption across the small intestinal epithelium and on the level of hepatic clearance.

For any *in vitro* model, detailed knowledge of actual culture composition and cellular phenotype is paramount for correct interpretation of data. A comprehensive view of cellular phenotype can be obtained with mass spectrometry-based proteomics, which today enables quantitative analysis of almost entire proteomes.[14] In this thesis, proteomic analysis and supportive functional studies were used to improve the understanding and applicability of important *in vitro* systems for predictions of drug disposition in the human small intestine and liver.

The human small intestine

The small intestine is the main site of absorption for an orally administered drug.[15] It is the longest part of the gastrointestinal tract, with a mean length of around 5 m,[16] and is divided into three distinct parts: the duodenum, the jejunum, and the ileum, with specialized roles in different aspects of absorption. The innermost layer of the small intestine is called the mucosa, and consists of epithelial cells resting on the lamina propria, a connective tissue scaffold that contains capillaries and nerve fibers, in turn supported by a layer of smooth muscle (the muscularis mucosa).[17]

The epithelium constitutes the main barrier between the intestinal lumen and blood.[18] Over 80% of the cells in the epithelium are enterocytes, which are highly polarized cells with distinct apical and basolateral membranes, and mainly responsible for the absorptive functions of the intestine.[19,20] The remaining part consists of mucus-secreting Goblet cells, hormone-producing enteroendocrine cells, and Paneth cells, which secrete various antimicrobial molecules.[19] The cells of the epithelium are organized in finger-like projections called villi, which are surrounded by glandular crypts.[17] The crypt-villus unit is a highly dynamic structure, where enterocytes are constantly being replenished in a conveyor-belt-like fashion through division of stem cells in the

crypt. As they migrate upwards along the crypt-villus axis, enterocytes trans-differentiate through a series of distinct functional stages.[21] At the villus tip, the cells finally undergo apoptosis and slough off into the intestinal lumen, typically around 4-5 days after their emergence from the crypt.[22,23]

Villi significantly increase the intestinal surface area and thus its absorptive capacity. The surface area is even further increased by the presence of microvilli on the apical membrane of epithelial cells (the brush border). Together, villi and microvilli provide a surface area enlargement of 60-120 times.[24]

The human liver

The liver is the largest internal organ in the human body, and the most important organ for the elimination of drugs and other xenobiotics from the bloodstream. Compounds that are absorbed in the small intestine first enter the hepatic portal system, and thus have to pass through the liver before reaching the systemic circulation. This is known as the hepatic first-pass effect, which can considerably decrease the bioavailability of extensively metabolized drugs. The efficiency of the liver in drug elimination is due in part to its highly vascularized nature, receiving up to a third of the total blood volume at any given time.[25] In addition to its involvement in metabolism and elimination, other vital functions of the liver include the synthesis and secretion of blood and bile constituents.[26]

Cellular organization and structure

The liver is primarily composed of parenchymal hepatocytes, which represent 60-70% of the total liver cell population, and as much as 80% of the liver volume.[13,27] Hepatocyte function is supported by several different types of NPCs, notably liver sinusoidal endothelial cells (LSEC), tissue-resident macrophages called Kupffer cells (KC), and vitamin A-storing hepatic stellate cells (HSC). Of these, LSEC are the most abundant, followed by KC and HSC. Being much smaller than hepatocytes, NPCs represent only 6.5% of the liver volume.[13]

On a microarchitectural level, hepatocytes are organized in linear plates throughout repeating structural units termed lobules (Figure 2). Lobules are basically hexagonal columns of cells that measure around 1 mm in diameter in humans.[28,29] Blood flows into the lobule from branches of the hepatic artery and portal vein, with 75% of the blood supply constituted by venous blood from the gastrointestinal tract.[30] Together with a bile duct, the hepatic artery and portal vein constitute a portal triad, with one such node at each corner of the lobule. Blood from the two different sources combines in sinusoidal blood vessels running between the hepatocyte plates, and finally drains in a central vein in the midpoint of the lobule.

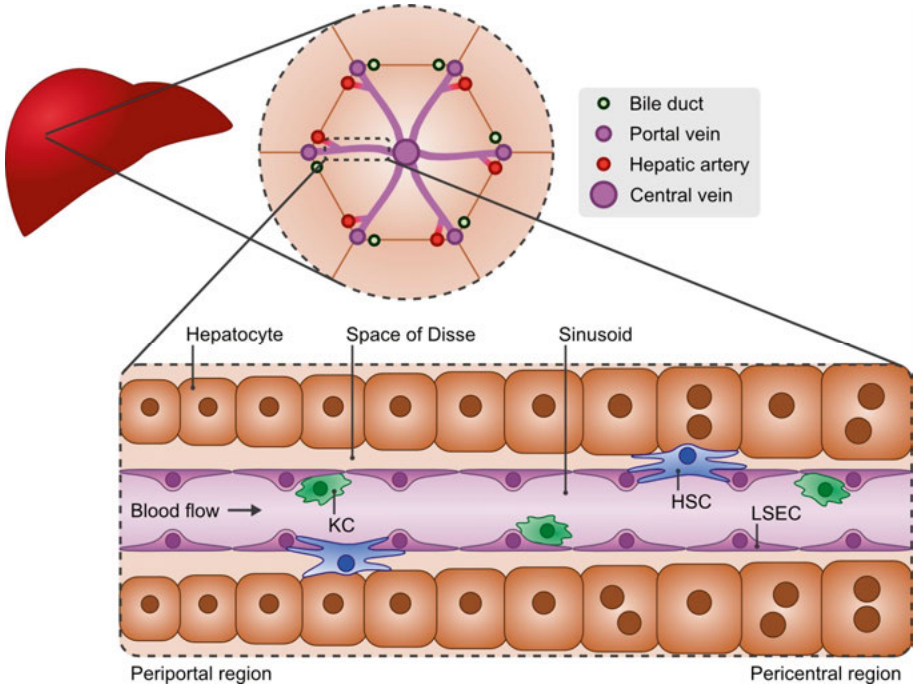

Figure 2. Microarchitectural organization of the liver. The liver is organized in repeating hexagonal units called lobules, made up of linear plates of hepatocytes. Blood from the hepatic artery and portal vein enters the lobule at each corner and flows through sinusoidal blood vessels to drain in a central vein. Hepatocytes show substantial differences in size, ploidy, and expression along the porto-central axis. The sinusoids are lined by fenestrated liver sinusoidal endothelial cells (LSEC) that give hepatocytes direct access to blood components. Kupffer cells (KC), specialized liver-resident macrophages, adhere to the inner surface of the endothelial wall. The perisinusoidal space of Disse, between LSEC and hepatocytes, contain pericyte-like hepatic stellate cells (HSC).

Hepatocytes

Hepatocytes are highly specialized epithelial cells that are responsible for most aspects of liver function, including the elimination of xenobiotics.[26] In terms of the biochemical and physiological functions they perform, hepatocytes show considerable spatial heterogeneity along the porto-central axis of the liver lobule (Figure 2), which is known as liver zonation.[12] This heterogeneity results from the polarized nature of hepatic blood flow, where cells in the periportal region consume and secrete various factors and thereby establish concentration gradients towards the downstream pericentral region.[31] Particularly notable is the difference in oxygen tension, which drops markedly as blood flows towards the central vein, reaching less than half of circulatory levels.[32,33] Furthermore, gradients in the concentrations of signaling molecules, such as Wnt morphogens and glucagon, are significantly involved in

the establishment of liver zonation,[34,35] and epigenetic differences in DNA methylation patterns have been suggested to form an additional layer of regulation.[36]

Many central liver functions show distinct zonation profiles. Among the most well described zonated processes, whose zonation have been known for decades, are different types of hepatic metabolism, notably of carbohydrates,[37] nitrogen,[38] and drugs.[39] In more specific terms, gluconeogenesis and urea synthesis are mainly performed by periportal hepatocytes, while pericentral hepatocytes are highly active in glycolysis and drug metabolism.[12] More recently, comprehensive single-cell RNA sequencing (RNA-seq) studies have revealed that as many as half of all genes expressed in hepatocytes are zonated.[40,41] An important point brought up by these studies is that most zonated processes are not binary, i.e. on or off in periportal and pericentral hepatocytes, but rather gradually changing across the porto-central axis.

A final aspect of note in the context of hepatocyte heterogeneity is that functional zonation is accompanied by differences in cell morphology, size, and ploidy (Figure 2). Thus, periportal hepatocytes are typically small and diploid, whereas pericentral hepatocytes are large, polyploid, and sometimes even multinucleated.[42-44] The cells also vary across the lobule in terms of their organelle content.[45] For instance, there are regional differences in the amounts of smooth and rough endoplasmic reticulum (ER), and pericentral hepatocytes contain higher numbers of mitochondria.[46]

Non-parenchymal cells

The walls of hepatic sinusoids are lined by LSEC. These thin, elongated cells contain numerous small pores, or fenestrations, with diameters of approximately 100 nm in humans,[47] through which many blood components can freely diffuse into the perisinusoidal space of Disse between LSEC and hepatocytes. The fenestrations, which cover around 9% of the surface area of LSEC,[48] facilitate direct contact between the blood and the liver parenchyma, which enhances the ability of hepatocytes to efficiently clear drugs and other xenobiotics from the blood.[26] In addition to their structural role, LSEC use their significant endocytic capacity to act as a scavenger system for clearance of macromolecular waste products originating from normal tissue turnover, and participate in liver immunity.[49]

The sinusoids are also the site of residence for KC, which constitute 80-90% of the total macrophage population in the body.[50] KC have a high capacity for endocytosis and phagocytosis, and are the first cells to encounter and process materials that arrive from the gastrointestinal tract, such as food antigens and microorganism-derived products. Another important function of these cells is the capture and elimination of blood-borne pathogens during systemic infections.[51,52] Their strategic location in the sinusoids give KC a key

role in immune surveillance and in initiating an orchestrated immune response, including the recruitment of other immune cells from the blood.[53] Apart from these protective functions, KC are sometimes involved in mediating liver damage caused by hepatotoxic compounds, most often through the release of cytokines and other inducers of hepatic cell death triggered by the offending compound.[54,55]

Completing the cell composition of the liver lobule are HSC, which reside within the perisinusoidal space of Disse and physically embrace the LSEC in a pericyte-like manner through extensive cytoplasmic projections.[56] Among the most prominent functions of quiescent HSC under normal physiological conditions are vitamin A (retinol) storage, where their lipid droplets contain 80% of total body retinol, and the control of extracellular matrix (ECM) homeostasis, via the balanced secretion of ECM proteins and ECM-degrading enzymes.[56] During liver injury, HSC leave their quiescent state and undergo an activation process to acquire a myofibroblastic phenotype, characterized by loss of vitamin A droplets and highly increased secretion of ECM components. In this way, activated HSC significantly contribute to the pathogenesis of liver fibrosis.[26,57]

Small intestinal and hepatic drug disposition

The disposition of drugs within and across epithelia is affected by several distinct pathways and obstacles. Cellular membrane barriers are always involved, which can be crossed via different pathways. Broadly, these pathways are either passive (driven by concentration gradients across membranes) or active (carrier-mediated), and, together with hepatic metabolism, determine the amount of an orally administered drug that can reach the systemic circulation (Figure 3).

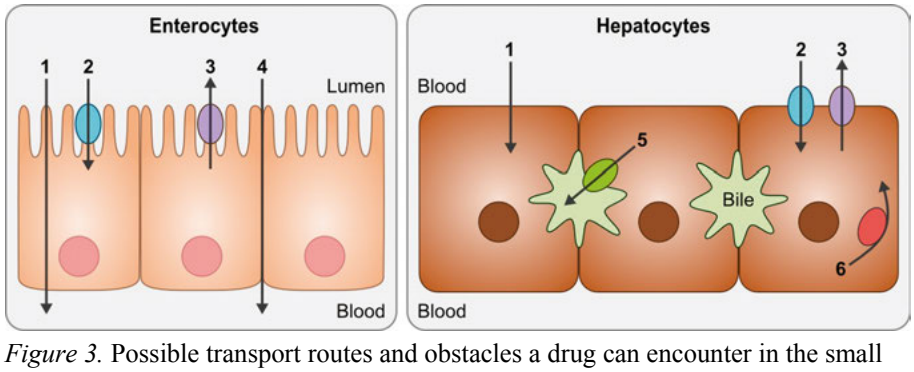

Figure 3. Possible transport routes and obstacles a drug can encounter in the small intestine and liver before reaching the systemic circulation. 1, passive transcellular (or lipoidal) diffusion; 2, carrier-mediated uptake transport; 3, carrier-mediated efflux transport; 4, passive paracellular diffusion; 5, bile excretion; 6, hepatic metabolism.

Transcellular diffusion

For many drugs, passive lipoidal diffusion via the transcellular pathway, i.e. passage through cells, is considered to be the primary route of cellular uptake and permeation through the small intestinal epithelium.[58-60] Since the lipid bilayers of cell membranes are hydrophobic structures, transcellular diffusion of a drug molecule is highly dependent on its lipophilicity and molecular size.[58] Diffusion rates differ between the basolateral and apical enterocyte membranes, however, and the apical membrane is usually considered to be the rate-limiting barrier for intestinal drug absorption, likely due to its lipid composition.[61]

Paracellular diffusion

Cells in epithelial tissues are joined together by tight junctions. Tight junctions are protein structures that maintain tissue integrity and help regulate the passage of solutes across the epithelial barrier.[62] These structures create pores in the epithelium, which can contribute to passive intestinal drug absorption through so-called paracellular diffusion, i.e. passage between cells.[63,64] For most drugs, this contribution is limited, but the paracellular pathway may be significantly involved in the absorption of some small and hydrophilic compounds.[65,66]

Carrier-mediated transport

In addition to passive diffusion, drug transport across membranes can be mediated by transport proteins, i.e. carriers.[67] Depending on the direction of transport, these proteins are classified as either uptake or efflux transporters. As their names imply, the activity of uptake transporters lead to increased membrane permeation of affected substrates, while efflux transporters generally limit permeation and cellular exposure,[68] and participate in hepatic drug elimination.

The human genome contains over 400 membrane transporters, belonging to two major superfamilies: the solute carrier (SLC) family, primarily comprising uptake transporters, and the ATP-binding cassette (ABC) family of efflux transporters, with 395 and 49 known members, respectively.[69,70] The expression of SLC and ABC transporters is highly heterogeneous throughout the human body,[71,72] meaning that the contribution of carrier-mediated transport to drug disposition can vary across organs.[73] Accordingly, enterocytes and hepatocytes express different panels of transporters that are important to study in drug development, due to their involvement in pharmacokinetics, drug-drug interactions, and liver toxicity (Figure 4).[67,74,75]

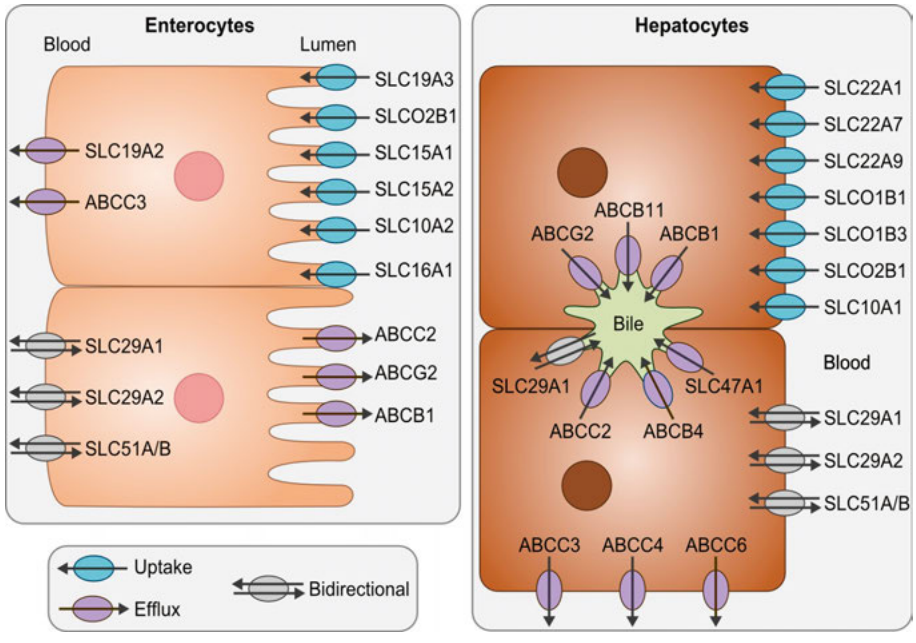

Figure 4. Membrane transporters of importance in drug development. The figure shows enterocyte and hepatocyte expression of drug disposition-related members of the SLC and ABC superfamilies. Adapted from a schematic drawing by the International Transporter Consortium.[75]

Hepatic metabolism

Another obstacle that comes into play after drug uptake into hepatocytes, whether it be through passive or active mechanisms, is hepatic metabolism. In broad terms, hepatic drug metabolism is divided into two phases. In phase I, drug compounds are converted into more polar metabolites, which can then be conjugated with endogenous charged species in phase II.[76] These metabolic processes generally transform the parent compound into more easily excretable forms.

The major enzymes in phase I metabolism are the cytochromes P450 (CYPs), of which many are highly expressed in the liver. Together, the most important CYPs are involved in the metabolism of 70-80% of clinically used drugs.[77] Major families of phase II enzymes include the UDP-glucuronosyltransferases (UGTs), sulfotransferases (SULTs), and glutathione S-transferases (GSTs).[78]

Hepatotoxicity

Due to its central role in drug metabolism and elimination, the liver is at a higher risk of exposure to toxic compounds than any other organ.[79] In fact, drug-induced liver injury (DILI) is one of the most common causes for the

withdrawal of an approved drug from the market.[79-81] Some types of DILI are predictable and dose-dependent (intrinsic DILI), but the more problematic form, referred to as idiosyncratic DILI, is highly unpredictable and typically occurs after a long latency period.[82]

The toxicity of a drug, or its metabolites, is initiated by hepatocyte stress, usually caused by mitochondrial dysfunction, accumulation of reactive oxygen species (ROS), or disruption of bile acid homeostasis.[82,83] In intrinsic DILI, this stress triggers the induction of cell death mechanisms, primarily apoptosis and necrosis, which directly lead to hepatocyte demise.[84] Idiosyncratic DILI can be initiated by similar mechanisms, but is also widely believed to involve the activation of innate and adaptive immune response mechanisms.[82,84]

In vitro methods for studies of small intestinal and hepatic drug disposition

As alluded to above, *in vitro* models for determining small intestinal and hepatic drug disposition are key elements of the drug development process. Many models that simulate the functions of these organs exist, with varying degrees of complexity. For the small intestine, the most important parameter to evaluate is drug absorption, and models that simulate its function therefore typically consist of some sort of barrier (artificial or cell-based) that separates two different buffer compartments.[85] Drug absorption can then be estimated by following the drug flux across the barrier. For the liver, important properties to study include drug uptake, metabolism, and toxicity. This can be done in a variety of culture configurations, using primary hepatocytes or different hepatocyte-like cells.[86] Some prominent *in vitro* models for small intestinal and hepatic drug disposition are described in more detail below.

In vitro models of the small intestine

One of the simplest ways of analyzing small intestinal drug absorption through passive diffusion *in vitro* is to use artificial lipid membranes, where an organic solvent containing phospholipids and other membrane constituents is added onto a filter support.[85] The drug (in a buffer solution) is added to the apical side of the membrane, and its time-dependent appearance in the basolateral compartment is monitored. Methods based on this approach are called parallel artificial membrane permeability assays (PAMPA), in reference to its first implementation.[87] PAMPA assays facilitate high throughput, and have shown reasonable correlations with the fraction of dose absorbed in humans.[88] However, they do not provide any information on carrier-mediated transport, for which more sophisticated, cell-based models are necessary.

Cell-based models for drug absorption studies, although similar to PAMPA in layout, use a cell monolayer in place of an artificial membrane (Figure 5). One of the most commonly used models in this context is the Caco-2 cell line. Caco-2 cells originate from a human colon carcinoma[89] and spontaneously differentiate to acquire an enterocyte-like phenotype, with tight junctions and polarized membranes, when cultured on permeable filter supports.[1,90,91] Results from Caco-2 experiments have been shown to strongly correlate with human *in vivo* data for drugs that are absorbed by passive transcellular diffusion,[92] and they can provide information on carrier-mediated transport as well, due to the expression of some transport proteins.[93] Estimating paracellular transport is more problematic, however, as the tight junctions in a Caco-2 monolayer are less porous than in the small intestinal epithelium.[94]

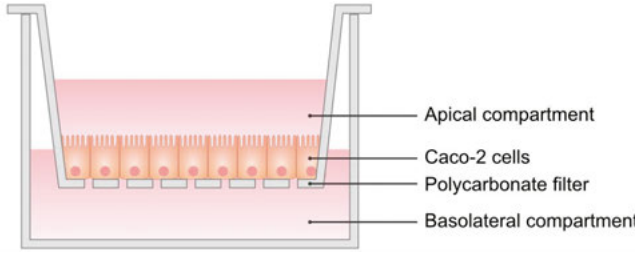

Figure 5. Configuration of a typical Caco-2 culture. Caco-2 cells are cultured on a polycarbonate filter support that separates an apical compartment (corresponding to the small intestinal lumen) and a basolateral compartment (corresponding to blood).

Another problem with Caco-2 cells relates to their cancerous origin. Cancer cell lines are, as a rule, inherently unstable and highly prone to genetic drift.[95,96] Careful control over culture conditions and passage numbers therefore needs to be exerted, as illustrated by the differences observed in an inter-laboratory comparison of data obtained from Caco-2 experiments.[97] Notable alternatives to Caco-2 cells include Madin-Darby canine kidney (MDCK) and LLC-PK1 cells (derived from canine and porcine kidney epithelium, respectively),[85] which form polarized monolayers and are readily transfected with specific transporters,[98] and the human colon cell line HT29, which can be induced to differentiate into either absorptive or mucus-secreting cells.[85]

An even more *in vivo*-like model for drug absorption studies is the Ussing chamber. Perhaps best described as an *ex vivo* model, the Ussing chamber consists of a piece of excised epithelial tissue mounted between two buffer compartments.[99] This method is best used for in-depth secondary screening, as it does not allow the same throughput as PAMPA or cell-based methods.[85]

In vitro models of the liver

Primary human hepatocytes constitute the gold standard *in vitro* model for studies of hepatic drug disposition and toxicity.[86,100-102] Human hepatocytes

are typically isolated using a two-step collagenase perfusion protocol, with starting material obtained from multi-organ donors or from patients undergoing liver resection surgery for tumor removal.[103-106] Hepatocytes can be used in different culture configurations, where the choice depends on the research question as well as various practical considerations, such as the required culture time and the availability of suitable detection methods. Some notable examples of hepatocyte culture configurations are described below (Figure 6). Most researchers rely on cryopreserved cells for their experiments, due to the relative ease with which they can be obtained. In fact, the decades of research put into optimization of cryopreservation conditions[107,108] have enabled the use of cryopreserved hepatocytes for many applications that were the exclusive domain of freshly isolated cells in the past,[109,110] even if problems with variable attachment properties after thawing still remain.[8-11]

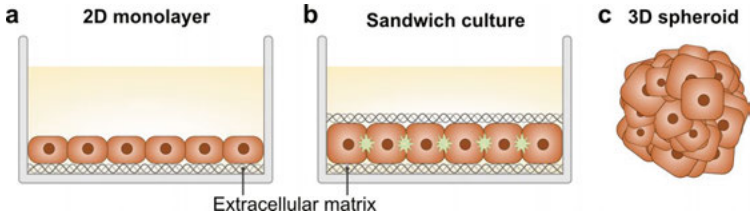

Figure 6. Examples of culture configurations for studies of hepatic drug disposition and toxicity using human hepatocytes. (a) Conventional 2D monolayer, where hepatocytes are cultured on a surface coated with ECM proteins. (b) Sandwich configuration, in which a second layer of ECM is added on top of the cells. (c) 3D spheroid culture, where hepatocytes aggregate to form small spheroidal microtissues.

Apart from suspension culture, which can only be used for very short-term experiments (since anchorage-dependent cells cannot live long without survival signals from ECM interactions),[111,112] the simplest way to culture hepatocytes is as conventional 2D monolayers (Figure 6a).[113] Hepatocytes do not readily adhere to plastic, however, and culture vessels are therefore typically coated with collagen to facilitate attachment.[26] As an example of their utility, hepatocyte monolayers can be used for evaluating the metabolic stability of drugs for several hours up to a couple of days.[114] During that time, however, hepatocytes undergo considerable dedifferentiation and eventually lose the ability to perform many liver-specific functions, including drug transport and metabolism.[4-6]

One way to overcome the problems with conventional 2D monolayers is to add a second layer of ECM on top of the cells, forming a so-called sandwich culture (Figure 6b).[86] In this configuration, the cells can form cell-matrix interactions in all directions, which better resembles the *in vivo* situation. This results in substantial improvements in cell morphology and liver-specific function, including the re-formation of bile canaliculi,[115,116] which enables

studies of canalicular efflux.[117,118] Hepatocytes in sandwich culture can remain functional for considerably longer periods of time than in 2D monolayers.[115]

Another way to increase the stability and physiological relevance of hepatocytes *in vitro* is to let them self-aggregate into spheroidal microtissues termed spheroids (Figure 6c).[119] Hepatocyte spheroids obtain a three-dimensional architecture, with cell-cell contacts on all sides, and deposit their own ECM material to essentially encapsulate the entire structure.[120] This *in vivo*-like organization enables maintained survival and functionality for extended periods of time (several weeks),[86,119] with high degrees of physiological relevance at the transcript, protein, and metabolite levels.[102,121,122] Spheroids can be generated in multiple ways, but the most prominent methods are gravity-enforced self-assembly in hanging drops[123] and culture on low-attachment surfaces.[121,124] A distinct advantage with spheroid culture is the small number of cells it uses, often requiring only a few thousand cells per well.

Alternative sources of cells for *in vitro* studies of hepatic drug disposition and toxicity include hepatoma cell lines, such as HepG2[125] and HepaRG,[126] as well as various stem cell-derived hepatocyte-like cells,[86] which are all readily available and relatively inexpensive. To date, however, none of the alternatives offer the levels of *in vivo* relevance achieved with primary hepatocytes.[26,86,119]

Mass spectrometry-based global proteomics

Technological progress in label-free mass spectrometry-based proteomics over the last years has now enabled the quantitative analysis of virtually entire proteomes.[14] Analysis of global gene expression (i.e. transcriptomics) has been possible for a longer time, but it is well known that RNA and protein levels do not show perfect correlations.[127-129] The advent of global proteomics is thus highly advantageous for improved phenotypic understanding, as proteins are produced downstream of transcripts (Figure 7) and can describe cellular function and status in more detail.[130]

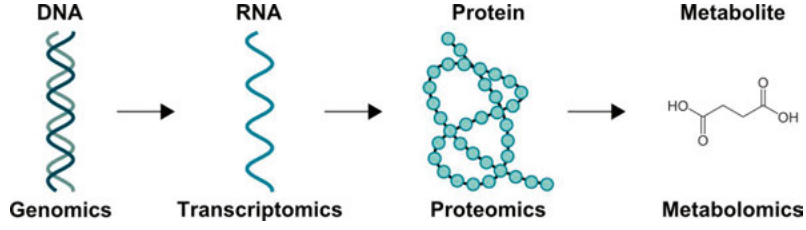

Figure 7. The flow of biological information. The measured molecules at each level are shown above the drawings, and the corresponding 'omics' technologies are denoted below.

Most strategies for proteomic analysis are so-called bottom-up approaches, where proteins are subjected to proteolytic digestion into peptides, commonly with trypsin, before analysis.[131] Historically, label-free proteomics methods have not been considered to provide as accurate quantification as targeted approaches based on labeled peptide standards,[132] but developments in sample preparation and data processing, together with enhanced instrument sensitivity, now allow label-free quantification with a sensitivity that approaches targeted methods.[133] This has enabled large-scale proteomics efforts to map the proteome composition of almost all organs in the human body.[134-136] However, the proteome is highly dynamic and can rapidly change in response to external stimuli,[137-139] meaning that steady-state protein levels do not necessarily reflect alterations induced by cellular damage or disease.[140] Depending on the research question, analysis of context-specific samples may therefore be necessary. Regarding the liver and hepatocytes, for example, proteomics has been applied to study the effects of hepatocyte isolation,[141] cytostatic treatment,[142] and culture-induced dedifferentiation.[4]

Pathway analysis

Proteomics (and other 'omics' technologies; Figure 7) generates huge amounts of complex data, and drawing biologically meaningful conclusions from this data can be a daunting task.[143] A powerful way to approach this analytical task is to use pathway analysis, which essentially reduces analytical complexity by grouping proteins into biological pathways.[144] Pathway information exists in a growing number of knowledge bases, such as the Kyoto Encyclopedia of Genes and Genomes (KEGG),[145] Reactome,[146] and PANTHER[147] databases. This information can, in turn, be accessed and utilized with a plethora of different data analysis tools.[144,148]

The first step in a typical pathway analysis (so-called overrepresentation analysis) is usually to identify a list of interesting proteins based on some application-dependent criterion, such as differential expression between two conditions, or cell-type-specific proteins in a comparison of different cell types. The proteins in the input list that belong to a certain pathway are then counted, and compared to the proportion of proteins from that pathway in a background list (e.g. the full proteome).[144] Finally, statistical methods are applied to test whether each pathway is over- or underrepresented in the list of input proteins.[144] This generates a condensed, less complex set of results, which facilitates interpretation as well as visualization.

Aims of the thesis

The overall aim of this thesis was to use mass spectrometry-based proteomic analysis, together with functional studies, to improve the understanding and applicability of important *in vitro* model systems for studying small intestinal and hepatic drug disposition.

The specific aims were:

- To analyze the proteome of filter-grown Caco-2 cells, and assess the impact of expression differences between the cell line and human jejunum on *in vitro*-*in vivo* extrapolations in drug transport studies (Paper I).

- To investigate and ameliorate the problem of variable attachment efficiency triggered by cryopreservation of human hepatocytes, and to study the characteristics and functionality of 'rescued' cells (Paper II).

- To evaluate the utility of quantifying cell debris particles in bright-field microscopy images as a novel apoptosis detection method (Paper III).

- To investigate the size characteristics of isolated human hepatocytes, and to assess whether size separation can be used to study zonated liver functions *in vitro* (Paper IV).

- To analyze the proteomes of human hepatocytes and the major types of liver NPCs, for improved understanding of the functional roles of different cell types (Paper V).

Methods

Proteomic analysis

The proteomes of the cell systems investigated in papers I, II, IV, and V of this thesis were analyzed by high-resolution, quantitative liquid chromatography-tandem mass spectrometry (LC-MS/MS). After sample collection, cells were lysed in a buffer with a high concentration of SDS. Cell homogenates, containing solubilized proteins, were processed in ultrafiltration units with the multi-enzyme digestion filter-aided sample preparation (MED-FASP) protocol.[149] Protein and peptide amounts were measured with a tryptophan fluorescence assay.[150]

Peptide mixtures were analyzed on LTQ Orbitrap and Q Exactive HF mass spectrometers. The resulting MS data was analyzed with the MaxQuant software for automatic identification and quantification of proteins.[151] Protein concentrations were calculated with the total protein approach (TPA), which assumes that the summed peptide intensities in a sample represent the total protein content.[152] By dividing the intensity of peptides from a certain protein with the corresponding summed intensity, its fraction of the total protein mass in a particular sample can be used to calculate the concentration:

$$\text{Protein concentration} = \frac{\text{MS signal}}{\text{Total MS signal} \times M_w} \left[\frac{\text{mol}}{\text{g total protein}}\right] \qquad \text{(eq. 1)}$$

where ‘MS signal’ is the MS signal of peptides from a particular protein, ‘Total MS signal’ is the summed intensity of all peptides, and M_w is the molecular weight of the protein in question. Protein copy numbers were calculated using the proteomic ruler method, which is based on the proportionality of the MS signal of histone proteins to cellular DNA content:[153]

$$\text{Protein copies per cell} = \text{MS signal} \times \frac{N_A}{M_w} \times \frac{\text{DNA mass}}{\text{Histone MS signal}} \qquad \text{(eq. 2)}$$

where ‘MS signal’, again, is the MS signal of peptides from a particular protein, N_A is the Avogadro constant, M_w is the molecular weight of the protein, ‘DNA mass’ refers to the amount of cellular DNA (assumed to be 6.5 pg),[153] and ‘Histone MS signal’ refers to the summed intensity of the detected histone proteins.

Bioinformatic analysis

Proteomic datasets were processed and filtered with spreadsheet software and the Perseus platform.[154] Pathway analysis and biological characterization of selected protein groups were performed with different databases and software tools, depending on the application. These included the Ingenuity Pathway Analysis (IPA) software,[155] the Ontologizer software tool,[156] the PANTHER Classification System,[147] the Reactome Pathway Knowledgebase,[146] DAVID Bioinformatics Resources,[157] and the Funrich software.[158]

Caco-2 cells

Paper I concerned proteomic analysis of the human colon carcinoma cell line Caco-2, connected to uptake transport studies of the SLCO2B1 substrate pitavastatin. Cell culture and experiments were performed as described below.

Caco-2 culture

The cells were used at passage 95-105 and maintained at 37 °C, with 10% CO_2, in Dulbecco's modified Eagle's medium (DMEM) supplemented with nonessential amino acids. For proteomics, Caco-2 cells were cultured on Transwell polycarbonate filter supports for 21 days before excision of the filters for sample preparation. Transport experiments were performed with cells cultured in 24-well plates.

Pitavastatin transport in Caco-2 cells

To study pitavastatin transport, Caco-2 cells were washed and then incubated with a concentration series of the compound in Hank's balanced salt solution (HBSS) for 4 min. Transport was stopped by the addition of ice-cold buffer. The amount of accumulated compound was quantified with LC-MS/MS. Transport rates were calculated with a modified version of the Michaelis-Menten equation, including a linear diffusion term (P_{diff}).[159]

Simulation of jejunal permeability

A simplified mechanistic model was used to simulate the jejunal permeability of pitavastatin, incorporating Caco-2-based kinetic parameters for SLCO2B1-mediated transport across the apical membrane, together with bidirectional passive diffusion. Flux across the basolateral membrane was considered to be purely passive. The model comprised three compartments (intestinal, intracel-

lular, and blood), and was set to mimic a typical intestinal perfusion experiment in a 10 cm segment of the intestine.[160] SLCO2B1-mediated transport in the jejunum was scaled from the Caco-2 data based on expression differences between the two systems.

Human hepatocytes

Proteomic and functional studies of human hepatocytes isolated in our laboratory were performed in papers II, III, and IV. Procedures surrounding the isolation, culture, and use of these cells are described below.

Hepatocyte isolation

Liver tissue for hepatocyte isolation was obtained from human donors undergoing liver resection surgery at the Department of Surgery, Uppsala University Hospital, Sweden. The procedure was in accordance with the approval from the Uppsala Regional Ethical Review Board (Ethical Approval no. 2009/028). All donors provided their informed consent to tissue collection.

Hepatocyte isolation was performed based on a two-step collagenase perfusion protocol.[103] After flushing to remove blood, the tissue was transported to the laboratory in a hypothermic preservation medium (Hypothermosol FRS). Two blood vessels were cannulated, and medical adhesive was applied to the tissue surface for optimal perfusion. The tissue was submerged in warm DPBS before initiating perfusion. In the first perfusion step, a calcium-depleted buffer was used to disrupt cell-cell connections. In the second step, the connective tissue was digested by perfusion with a buffer containing a collagenase/protease mixture. After digestion was completed, cells were gently dispersed in warm medium and subjected to a series of washing steps, using low-speed centrifugation to remove dead hepatocytes and NPCs. The final washing step consisted of density centrifugation with Percoll, to obtain a preparation of highly viable hepatocytes.

Cryopreservation and thawing

Hepatocytes that were not used freshly after isolation were routinely cryopreserved for subsequent experimentation. Hepatocyte suspensions were adjusted to 10×10^6 viable cells/ml in cryopreservation medium containing fetal bovine serum (FBS), and 1 ml aliquots were added to cryovials. The cryovials were kept in isopropanol freezing containers at -80 °C for 2 h before transfer to long-term storage at -150 °C.

Thawing was performed by immersing cryovials in a 37 °C water bath for around 2 min. Cell suspensions were poured into 50 ml tubes filled with pre-warmed density gradient medium and centrifuged to decrease the presence of

non-viable cells. Finally, cell pellets were resuspended as appropriate for the intended application, as described below.

Hepatocyte culture

Freshly isolated or thawed hepatocytes were resuspended in DMEM supplemented with HEPES buffer, glucose, FBS, insulin, dexamethasone, l-glutamine, and penicillin-streptomycin (PEST). Cells intended for experiments in a suspension format were used immediately. For adherent monolayer culture, cells were seeded in collagen I-coated multiwell plates at a concentration of 0.75×10^6 cells/ml and incubated at 37 °C with 5% CO_2. After an attachment period of 3 h, the medium was replaced with hepatocyte maintenance medium supplemented with insulin, transferrin, selenium, dexamethasone, and PEST (complete HMM). Attachment efficiency was calculated as the percentage of initially seeded cells that were able to attach. For 3D spheroid culture, resuspended hepatocytes were seeded in 384-well ultra-low attachment plates at 5000 cells/well and incubated as above. After 48 h, 80% of the medium was aspirated and replaced with complete HMM. The medium was then exchanged every 48-72 h up to 21 days.

Evaluation of hepatocyte quality

Hepatocyte quality was evaluated with a morphological scoring metric (termed monolayer score) developed in paper II and further applied in paper IV. In brief, monolayers were imaged with an inverted microscope after 24 h in culture. Three experienced researchers were given de-identified, randomized images for assignment of an overall monolayer score of 1-4 (with higher numbers indicating higher quality), based on five morphological parameters: uniformity of cell shape, level of cell stretching, distinctness of cell boundaries, presence of dead cells and debris, and monolayer confluence. Final monolayer scores were obtained by taking the mean of individual assessments.

Size separation with counterflow centrifugal elutriation

Hepatocytes were resuspended in an ice-cold HBSS-based buffer, and filtered through a 70 µm cell strainer to remove large aggregates. The cell suspension was injected into a JE-5.0 elutriation rotor running in an Avanti J-20 XPI centrifuge, set up with the small elutriation chamber. The system was kept at 4 °C, and centrifugation speeds and buffer flow rates were gradually adjusted for sequential collection of six different size fractions. Samples for experiments were used immediately, and samples for proteomic analysis were stored at -80 °C.

Pitavastatin transport in hepatocytes

Hepatocytes were cultured as monolayers for 24 h. The cells were then incubated with a 1 μM solution of pitavastatin in HBSS for 10 min. The drug solution was aspirated and further transport was stopped by the addition of ice-cold DPBS. The amount of accumulated pitavastatin was quantified with LC-MS/MS.

Drug metabolism

In paper II, drug metabolism was assessed by adding a solution of diclofenac and midazolam (1 μM in HBSS) to hepatocyte monolayers cultured for 24 h. Diclofenac is a substrate for CYP2C9, and midazolam is a substrate for CYP3A4. Samples were collected at 0, 20, 40, and 60 min, after which the experiment was stopped by adding ice-cold acetonitrile. Compound degradation was measured with LC-MS/MS.

In paper IV, hepatocyte size fractions in suspension were incubated with two drug cocktails (in complete HMM) at concentrations of 1 μM for each drug. The first cocktail contained midazolam (CYP3A4), bufuralol (CYP2D6), bupropion (CYP2B6), amodiaquine (CYP2C8), and diclofenac (CYP2C9), and the second cocktail contained S-mephenytoin (CYP2C19) and phenacetin (CYP1A2). Incubations were performed for 90 min in total, and samples were collected after 0, 5, 10, 15, 20, 30, 60, and 90 min. Reactions were stopped by mixing with ice-cold acetonitrile/water (60:40). The amount of compound remaining at each time point was quantified with LC/MS-MS, and clearances were calculated with the substrate depletion method.[161]

Image cytometry

Cell counts and viabilities were routinely analyzed with image cytometry, by staining cell suspensions with fluorescent probes for live (acridine orange) and dead (propidium iodide) cells. Corresponding bright-field images were always acquired simultaneously with fluorescent images, and all images were stored for future reference. Since the method is image-based, it enables morphometric studies, which was utilized for size analysis of cells and cell-derived debris particles in papers II, III, and IV.

Detection of cell stress and apoptosis

In papers II and III, the effects of culture conditions and toxic compounds on cell stress and apoptosis induction in human hepatocytes were studied. For

this purpose, different assays were used as outlined below, depending on culture configuration and endpoint.

Oxidative stress

Oxidative stress was measured by staining hepatocytes with the fluorescent substrate dihydroethidium (DHE), which exhibits bright red fluorescence once bound to nucleic acids after being oxidized by ROS.[162] The cells were incubated with the compound for 30 min, and fluorescence intensity was measured with a plate reader.

Fluorescence-based apoptosis detection

For cells in suspension, apoptosis was measured with image cytometry, similarly to the viability assay described above, using fluorescently labeled markers for phosphatidylserine externalization (annexin V) and caspase activation. Importantly, the image cytometry-based annexin V assay used here has been shown to give comparable results to conventional flow cytometry,[163] one of the most commonly used tools for apoptosis detection.

For cells in adherent culture, the culture medium was supplemented with a fluorescent detection reagent for caspase activation, which allowed repeated measurements over time to follow temporal apoptosis induction. In this case, fluorescence intensity was measured with a plate reader. Further visualization of caspase activation was performed by confocal microscopy.

Quantification of cell debris

Paper III concerned the development of a novel method for apoptosis detection, based on the quantification of subcellular debris particles in bright-field microscopy images. Briefly, the method that was developed uses an automated ImageJ macro that performs a series of image processing steps. First, background noise is reduced and the image is converted into a binary (black and white) format. Second, debris particles are highlighted and counted, and data is obtained as a tab-separated text file. The method was applied on bright-field images captured in parallel with the fluorescence-based image cytometry analyses described in the sections above.

Results and discussion

The proteome of filter-grown Caco-2 cells (Paper I)

The work described in paper I concerned a proteomic mapping of Caco-2 cells cultured on polycarbonate filters for three weeks. Similar analysis had previously been performed for Caco-2 cells grown in a less physiologically relevant configuration (on conventional culture plastic),[164] but an in-depth analysis of filter-grown cells was lacking at the onset of this thesis. When cultured on filters, Caco-2 cells can be used to mimic functions of the small intestinal epithelium, which is, chronologically, the first important physiological barrier a drug compound encounters on its journey towards the systemic circulation.

Using MED-FASP and mass spectrometry-based label-free quantification, 8096 proteins were identified, spanning seven orders of magnitude in concentrations (Figure 8a). Principal component analysis (PCA) incorporating proteomic data on human colon[165] and jejunum (unpublished data) showed that Caco-2 cells were markedly different from the tissues, but were most similar to jejunum (Figure 8b). A comparison with cells grown on plastic showed that upregulated proteins in filter-grown cells were mainly involved in molecular transport and metabolism, i.e. important enterocyte functions, while cells grown on plastic retained a more cancer-like phenotype. These results comprehensively supported the decades-old notion that filter-grown Caco-2 cells differentiate to resemble small intestinal enterocytes.[90,91]

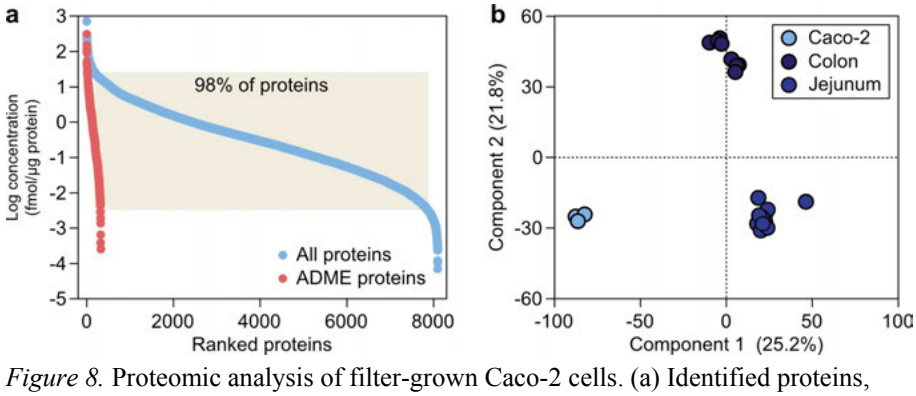

Figure 8. Proteomic analysis of filter-grown Caco-2 cells. (a) Identified proteins, ranked by concentration. ADME-related proteins are shown in red. (b) PCA of proteomic data from Caco-2 cells, and human colon and jejunum. Numbers in parentheses show the amount of data variability explained by each component.

Noteworthy is that the analysis gave near-complete coverage of proteins delineating enterocyte differentiation, including brush border enzymes, adherens and tight junction proteins, and ECM-interacting integrins. In terms of drug absorption properties, 112 SLC and 20 ABC transporters were detected, among which were nine of the 14 clinically relevant transporters present in enterocytes (SLCO2B1, SLC16A1, SLC15A1, SLC29A1, SLC51A/B, ABCB1, ABCC3, ABCC2, and ABCG2; Figure 9).

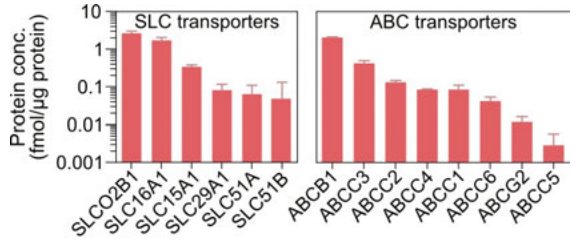

Figure 9. Protein concentrations of clinically relevant transporters in Caco-2 cells. Nine of the transporters are known to be present in enterocytes.[67,74,75]

More detailed studies were then performed for SLCO2B1, to assess the impact of *in vitro-in vivo* differences in protein expression. SLCO2B1 levels were 16-fold higher in Caco-2 cells than in jejunum (Figure 10a), which was used together with permeation kinetics to scale the transport velocity in simulations of time-dependent pitavastatin absorption at fixed concentrations.

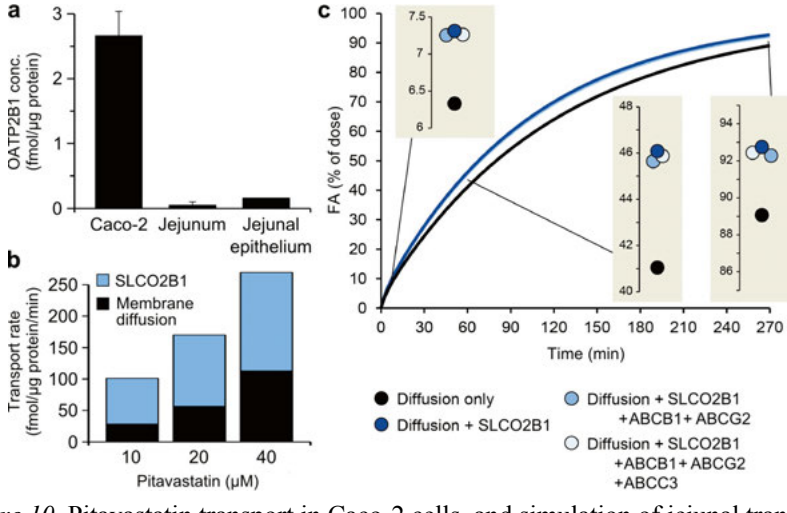

Figure 10. Pitavastatin transport in Caco-2 cells, and simulation of jejunal transport. (a) SLCO2B1 concentrations in Caco-2 cells and human jejunum, including data corrected for epithelial cell proportions. (b) Pitavastatin uptake via SLCO2B1 and passive diffusion in Caco-2 cells, at clinically relevant concentrations. (c) Simulation of pitavastatin absorption in human jejunum based on transport kinetics in Caco-2 cells and transporter concentration differences between Caco-2 cells and jejunum. The effect of selected efflux transporters is also shown.

It was found that SLCO2B1 contributed to around 60-70% of pitavastatin uptake in Caco-2 cells (Figure 10b), but the lower expression in jejunum led to a markedly lower predicted transporter contribution (<5%), suggesting that passive transcellular diffusion dominates pitavastatin absorption *in vivo* (Figure 10c). This discrepancy emphasizes the crucial importance of taking expression differences between cell models and actual tissue into account for *in vivo*-relevant interpretation of drug absorption data.

Post-thaw restoration of cryopreserved human hepatocytes (Paper II)

From paper II onwards, the focus of the thesis work was placed on the liver. In paper II, the underlying reasons for the highly variable quality of cryopreserved human hepatocyte batches (in terms of attachment and morphology) were investigated. This is a well-known problem,[10,108] and the ultimate goal of the study was to find a way to improve the situation.

Initial characterization of standard post-thaw properties, i.e. viability, attachment efficiency, and monolayer confluence, showed that the 14 included cryopreserved hepatocyte batches covered a wide range of qualities (Figure 11a-b). For instance, attachment efficiency and confluence spanned ranges of 55-95% and 60-100%, respectively.

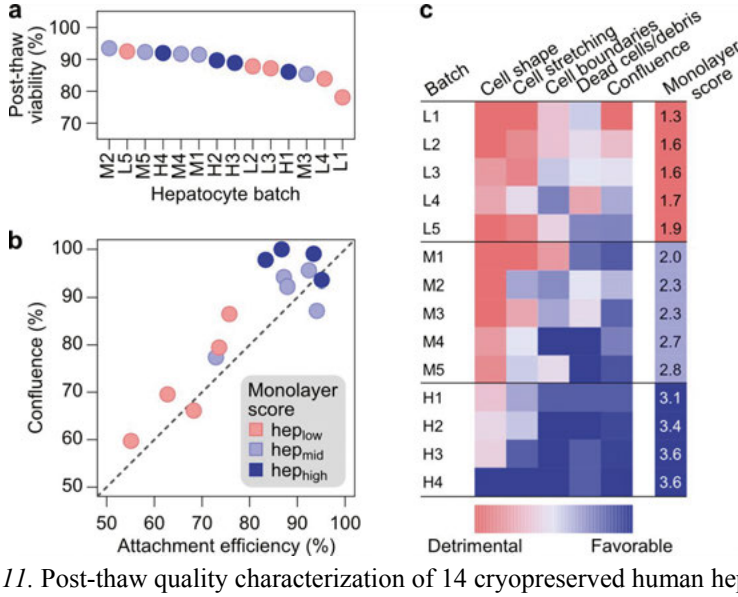

Figure 11. Post-thaw quality characterization of 14 cryopreserved human hepatocyte batches. (a) Cell viability immediately post-thawing. (b) Attachment efficiency and monolayer confluence, assessed after 3 and 24 h in culture, respectively. (c) Monolayer score classification of the batches, based on visual evaluation of cellular morphology.

However, a highly confluent monolayer can still consist of cells with poor, unhealthy morphology. This prompted the development of a novel morphological scoring metric (termed monolayer score), based on visual assessments of cell shape, cell stretching, cell-cell interactions, the presence of dead cells and debris, and confluence. Three quality groups were defined based on monolayer scores: hep_{low}, hep_{mid}, and hep_{high}, across which the batches were evenly divided (Figure 11c). This was found to give a more comprehensive view of cell quality, and was used throughout paper II and later applied on a larger set of batches in paper IV.

Next, attached and non-attached hepatocyte fractions were subjected to proteomic analysis to explore possible reasons for the failure to attach. The analysis included representatives from each quality group, and 4013 proteins were identified in total. PCA showed pronounced differences between attached and non-attached hepatocytes (Figure 12), and 896 proteins were present at significantly different concentrations. Pathway analysis revealed that non-attached hepatocytes had a phenotype characterized by considerable cell stress, including upregulation of glycolysis and, notably, marked apoptosis activation.

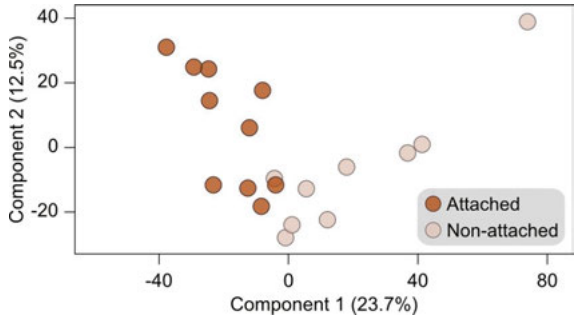

Figure 12. Proteomic analysis of attached and non-attached hepatocytes. Numbers in parentheses denote the amount of variability explained by each component in a PCA of the proteomic data.

The proteomic results formed the basis for more detailed analysis of cell stress and apoptosis. Staining with fluorescent markers confirmed that oxidative stress and apoptosis levels were significantly elevated in non-attached hepatocytes (Figure 13a-b). Additionally, hep_{low} batches, with generally lower levels of attachment, showed increased caspase activity already immediately after thawing (Figure 13c). The cells were then treated with various stress-reducing compounds during the standard 3 h attachment period, in an attempt to improve attachment efficiency. This post-thawing approach to attachment improvement has not been considered a worthwhile strategy to pursue.[109] Here, however, excellent results were obtained after blocking apoptosis with the pan-caspase inhibitor Z-VAD-FMK (Figure 14), which gave a dose-dependent increase in attachment efficiency (at 0-190 μM), with improved monolayer

morphology, and facilitated the formation of 3D spheroids, without affecting the hepatocyte proteome. The greater number of cells capable of attachment after Z-VAD-FMK treatment led to overall increases in hepatocyte functionality, in terms of uptake transport and drug metabolism.

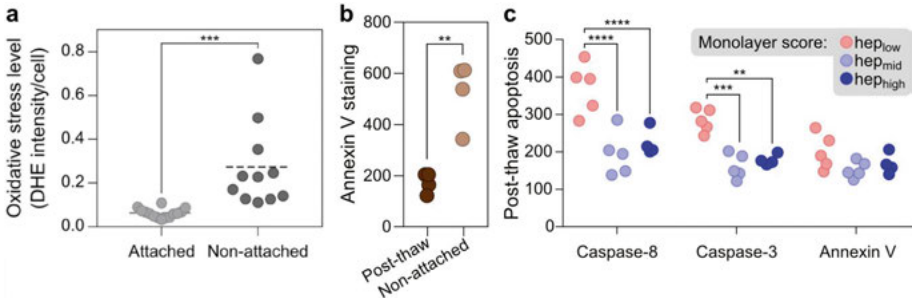

Figure 13. Cell stress and apoptosis in cryopreserved human hepatocytes. (a) Oxidative stress in attached and non-attached hepatocytes. (b) Annexin V staining in hepatocytes immediately after thawing and in non-attached cell fractions. (c) Post-thaw apoptosis levels in batches from different monolayer score groups, assessed by caspase activity and annexin V staining.

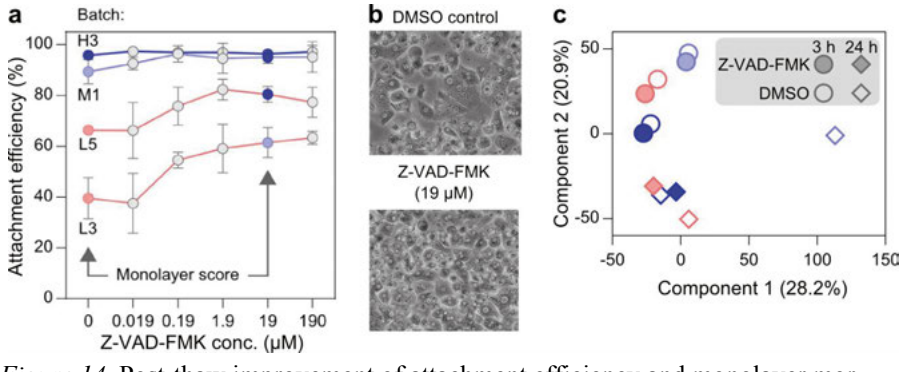

Figure 14. Post-thaw improvement of attachment efficiency and monolayer morphology. (a) Attachment efficiency of four hepatocyte batches after treatment with a concentration series of Z-VAD-FMK. Line colors indicate the baseline monolayer score group of each batch, and the colored dots show the monolayer score classification at 0 and 19 µM of the compound. (b) Monolayers from a hep_{low} batch treated with DMSO or 19 µM Z-VAD-FMK. (c) PCA of proteomic data from untreated cells and cells treated with Z-VAD-FMK for 3 h, analyzed after 3 and 24 h in culture. Numbers in parentheses denote the amount of data variability explained by each component.

Importantly, the treated cells remained responsive to apoptosis induction by celecoxib (as Z-VAD-FMK was rapidly washed away), showing that the treatment does not preclude the cells from use in hepatotoxicity testing. This simple treatment protocol can thus markedly increase the availability of human hepatocytes that are capable of attachment, which is a prerequisite for most applications in conventional as well as 3D culture configurations.

Apoptosis detection by cell debris quantification (Paper III)

While imaging hepatocyte suspensions during the work performed in paper II, it was observed that less viable (apoptotic) hepatocyte preparations contained higher levels of small debris particles. An ImageJ macro was developed to investigate the possibility of quantifying these debris particles in bright-field microscopy images as a simple measure of apoptosis. Around 70% of the detected particles had a diameter of 2-5 µm (Figure 15a), matching the size range of the apoptotic bodies that result from cell disintegration during apoptosis.[166]

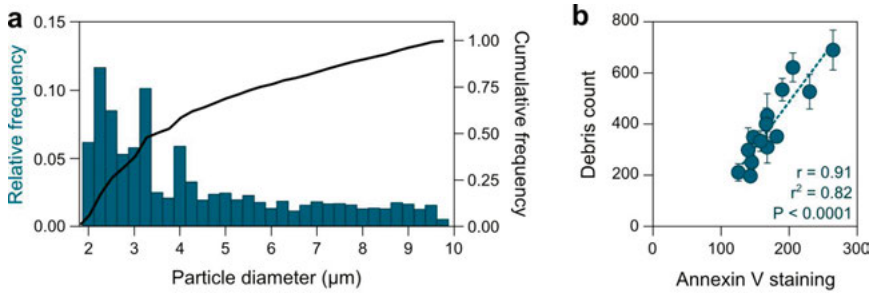

Figure 15. Image-based debris quantification as a measure of apoptosis. (a) Size distribution of debris particles in the 14 hepatocyte batches from paper II, shown as relative and cumulative frequencies. (b) Debris counts in the 14 batches correlated with annexin V staining. Error bars show standard deviations of technical quadruplicates. Annexin V staining is shown as size-normalized fluorescence intensity per cell.

The apoptosis results from the 14 batches in paper II were then compared with the corresponding debris counts. Debris counts were strongly correlated with annexin V staining of externalized phosphatidylserine (r = 0.91; Figure 15b), but only moderately correlated with caspase activation. This is consistent with the sequence of apoptotic events, where caspase activation precedes phosphatidylserine externalization, ultimately ending with cell disintegration.[166,167] In line with the results from paper II, non-attached cells showed elevated debris levels, which decreased dose-dependently after Z-VAD-FMK treatment (Figure 16), further confirming the primarily apoptotic origins of the debris.

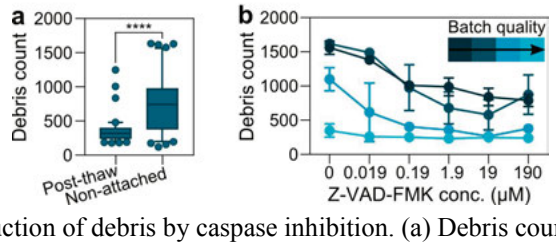

Figure 16. Reduction of debris by caspase inhibition. (a) Debris counts from 41 different experiments, post-thawing and in non-attached cell fractions. (b) Dose-dependent debris reduction in four batches after treatment with Z-VAD-FMK.

To test the applicability of the method, hepatocytes were cultured under non-adherent conditions (i.e. in suspension), which triggers apoptosis in anchorage-dependent cells (a phenomenon termed anoikis).[168] Annexin V staining and debris counts showed similar increases over a period of 7 h, demonstrating that temporal apoptosis activation can be tracked with debris counts. Next, caspase activity and debris counts were measured after treating hepatocytes and MDCK cells in adherent culture with toxic compounds. MDCK cells, which are used in studies of nephrotoxicity,[169] were included to investigate whether the method could be used for other cell types than hepatocytes. Notably, the apoptosis inducer celecoxib triggered rapid, concentration-dependent increases in both caspase activity and debris counts in hepatocytes as well as MDCK cells (Figure 17). Altogether, these results demonstrated the utility of debris quantification as an easy-to-apply method for apoptosis detection.

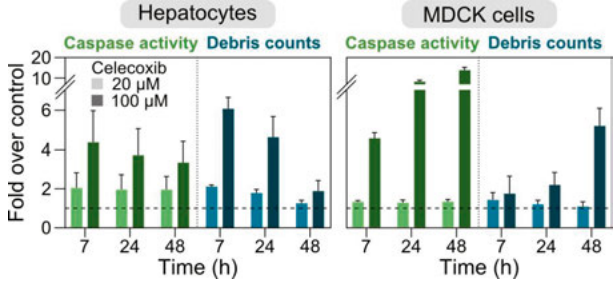

Figure 17. Celecoxib-induced apoptosis in adherent cultures of hepatocytes and MDCK cells. Apoptosis levels were measured by caspase activity and debris counts.

Liver zonation and cell size variability in human hepatocytes (Paper IV)

At the outset, the idea with paper IV was to perform retrospective analysis of the data collected during hepatocyte isolation and cryopreservation in the laboratory over the years. Along the way, however, certain interesting findings (described below) meant that the project expanded into an exploration of cell size variability and its association with liver zonation in isolated human hepatocytes *in vitro*.

As mentioned in the section on paper II, the monolayer score classification was here extended to include 50 batches (Figure 18a). It was found that more than half of the batches (54%) belonged to the hep_{high} group, and only six batches (12%) fell in the poor quality group (hep_{low}). Partial least squares (PLS) modeling was used to assess how donor background and various process parameters affected isolation and cryopreservation outcome (cell yield, viability, and monolayer score). No significant determinants were identified,

but an interesting trend was the influence of mean cell size, where high proportions of large cells reflected negatively on the isolation outcomes, but positively on monolayer scores (Figure 18b).

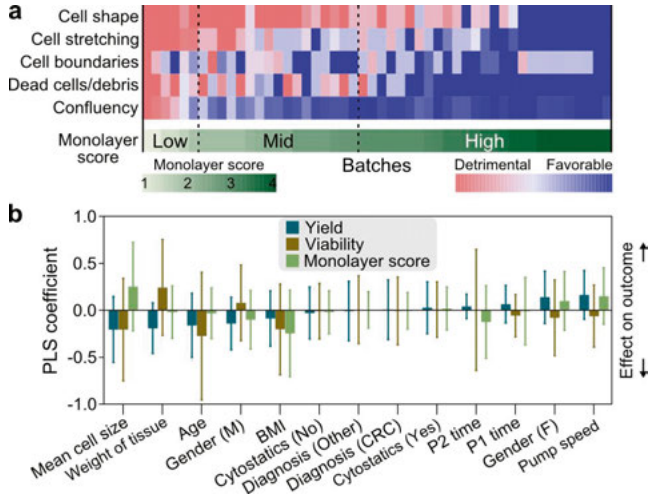

Figure 18. Isolation and cryopreservation of human hepatocytes. (a) Morphological evaluation of cryopreserved batch quality, using the monolayer score metric developed in paper II. (b) PLS modeling of the effect of differences in donor background and process parameters on the outcome of hepatocyte isolation and cryopreservation. Error bars show confidence intervals of the PLS coefficients.

The effects of cell size on isolation and cryopreservation outcome prompted an investigation of cell size variability across hepatocyte batches. On average, freshly isolated and cryopreserved batches had very similar size distributions (Figure 19a). However, considerable inter-batch variability was observed, with different distribution shapes and maxima that ranged from 14 to 22 µm in cryopreserved batches (Figure 19b).

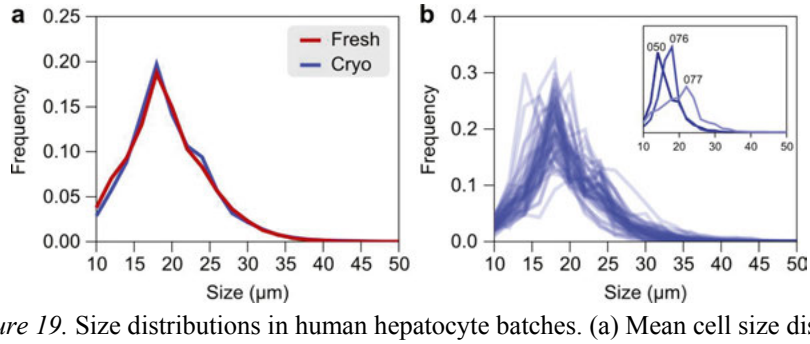

Figure 19. Size distributions in human hepatocyte batches. (a) Mean cell size distributions of freshly isolated and cryopreserved batches. (b) Size distributions in cryopreserved batches, showing the marked inter-batch variability. The inset panel shows examples of three highly different batches.

To probe the characteristics of hepatocytes of different sizes in more detail, counterflow centrifugal elutriation was used to separate hepatocytes from ten batches into six fractions of sequentially increasing size (Figure 20a). Mean size ranged from 15.8 ± 1.7 µm in the first fraction (F1) to 21.2 ± 3.7 µm in the last (F6). DNA content and multinucleation increased with increasing size (Figure 20b), in agreement with lobular structure.[42]

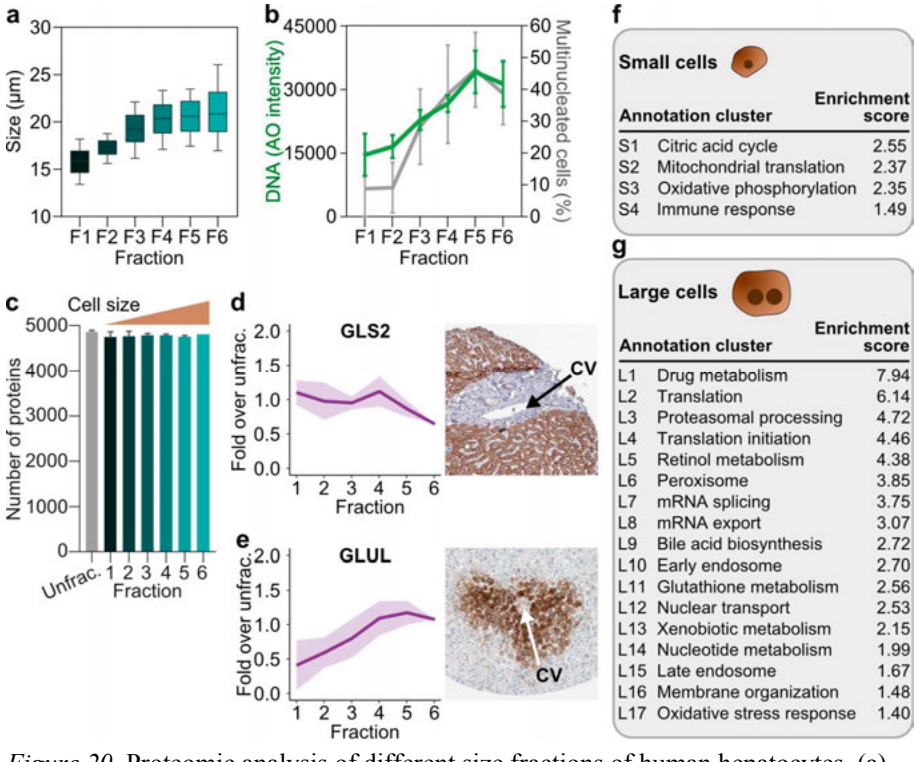

Figure 20. Proteomic analysis of different size fractions of human hepatocytes. (a) Cell size in six different size fractions obtained with counterflow centrifugal elutriation. (b) DNA content and multinucleation across size fractions. (c) Number of proteins that were detected in a proteomic analysis of the different size fractions. (d-e) Size-dependent expression of (d) the periportal marker GLS2 and (e) the pericentral marker GLUL, represented as fold over unfractionated controls. Shaded areas show standard deviations. Histological images from the Human Proteins Atlas (HPA)[170] show similar expression patterns. Arrows show central veins (CV). (f-g) Biological functions that were enriched in (f) small and (g) large hepatocytes.

Size fractions from three batches were analyzed with proteomics, and 5163 proteins were identified in total (Figure 20c). Glutaminase 2 (GLS2) and glutamine synthetase (GLUL), two well-known markers of liver zonation with predominant expression in the periportal and pericentral regions, respectively,[171] showed size-dependent expression patterns that matched the *in vivo* situation (Figure 20d-e).

Protein abundances in the different fractions were then correlated with fraction numbers (1-6), to find more proteins with sequentially enriched expression. Thresholds were set at Pearson correlation coefficients of -0.8 and 0.8 for enrichment in small and large hepatocytes, respectively. Thus, 151 proteins were enriched in small cells, and 758 proteins in large cells. Pathway analysis revealed that these proteins largely represented biological processes with known zonal specificity (Figure 20f-g). For instance, small hepatocytes showed enrichment of proteins involved in oxidative energy metabolism, while the most enriched function in large cells was drug metabolism.

To assess whether size-dependent expression differences would be reflected by similar functional differences, the activity of the seven most important CYP enzymes in hepatic metabolism[77] was analyzed in the different size fractions. Expression and activity across fractions were strongly correlated for four of the enzymes (CYP1A2, CYP2B6, CYP2C19, and CYP3A4; Figure 21), which were also the most clearly zonated in histological images from the HPA. In all, these results demonstrate that size separation of human hepatocytes can be used to study liver zonation *in vitro*.

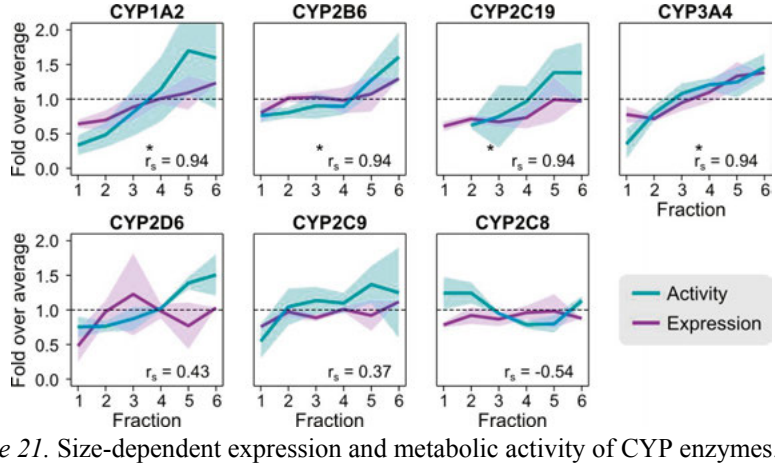

Figure 21. Size-dependent expression and metabolic activity of CYP enzymes. Both parameters are shown as fold over the average of all fractions. Shaded areas show standard deviations.

The proteomes of major cell types in the human liver (paper V)

As described in the introduction, the liver does not only contain hepatocytes, but also different types of NPCs that participate in many important aspects of liver function. A complete proteomic picture of the liver can thus not be obtained without analyzing these cells as well. Such analysis had previously been performed for murine liver.[172,173] However, the usefulness of rodent models

for understanding human biology is increasingly questioned,[174,175] and the goal of paper V was therefore to analyze the proteomes of the major human liver cell types, i.e. hepatocytes, LSEC, KC, and HSC, with a focus on proteins involved in the immune system and ADMET processes.

Matched samples of the four cell types from three histologically normal donors were obtained in collaboration with a commercial vendor. 9791 proteins were identified in total, of which around 53% were common to all cell types (Figure 22a). Data reliability was accentuated by the strong correlations among biological replicates for each cell type (mean Pearson correlation coefficients of 0.90-0.94). PCA showed that the four cell types all had distinctly different proteomes (Figure 22b). Further, a comparison with previously published murine data showed that there were pronounced species differences (Figure 22c).

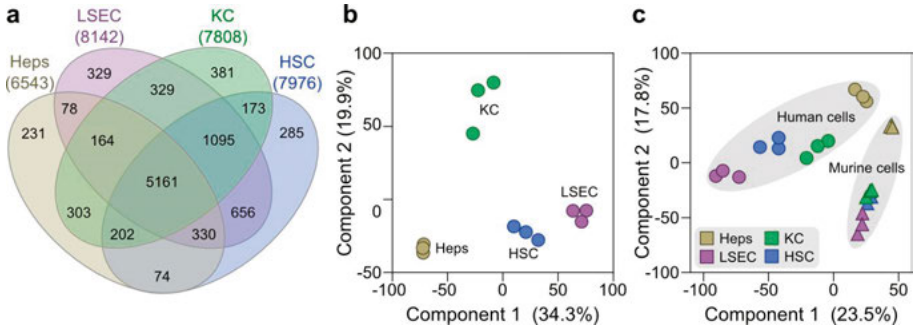

Figure 22. Proteomic analysis of major human liver cell types. (a) Number of identified proteins per cell type, and the overlap in protein identification between different cell types. (b) PCA of the proteomic data. The numbers in parentheses show the data variability explained by each component. (c) PCA comparing the proteomic data generated here with similar data from murine liver cells,[173] showing clear species differences.

As a benchmark of cell identity, the proteomic data on human liver cells was compared with transcriptomic data from a single-cell RNA-seq study of dissociated human liver cells.[41] The highest similarities were observed when comparing matching cell types, with RNA/protein correlations of 0.20-0.45 (Figure 23a).

The characteristics of cell-type-specific proteins were then studied, including proteins that were uniquely expressed in one cell type, or showed over 50-fold higher levels in one cell type compared to the others. Around 300-500 such proteins were found for each cell type (Figure 23b). Pathway analysis showed that they were enriched for biological processes representative of cell-type-specific functionality (Figure 23c). For instance, hepatocytes showed enrichment of proteins involved in various types of metabolism, many proteins specific to LSEC and KC were associated with the immune system, and HSC-specific proteins were related to the ECM.

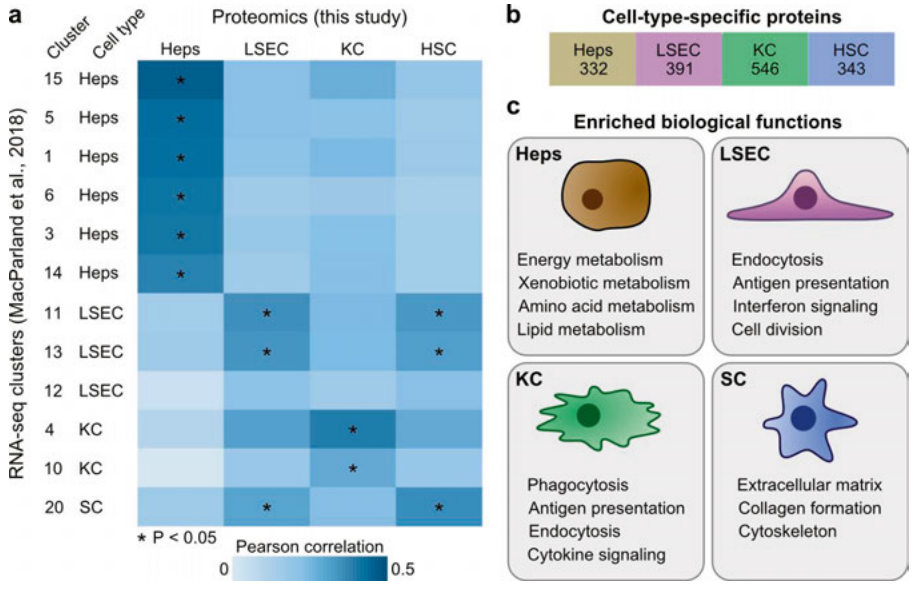

Figure 23. Benchmarking cell identity. (a) Protein concentrations in the samples from this project compared with corresponding RNA levels from a single-cell RNA-seq study.[41] Cluster numbers come from the RNA-seq study. (b) Numbers of cell-type-specific proteins in the four cell types. (c) Enriched biological functions among cell-type-specific proteins.

To explore the potential involvement of hepatocytes and NPCs in the pathogenesis of idiosyncratic DILI, the expression of selected categories of proteins with important immune-related functions was investigated. These included antigen presentation proteins, cytokine receptors, complement proteins, pattern recognition receptors (PRRs), and various alarmins. As could be expected, KC showed the most prominent overall expression of these proteins, in agreement with their role as tissue-resident macrophages. Taking antigen presentation as an example, major histocompatibility complex (MHC) class II molecules were exclusive to KC (Figure 24a).

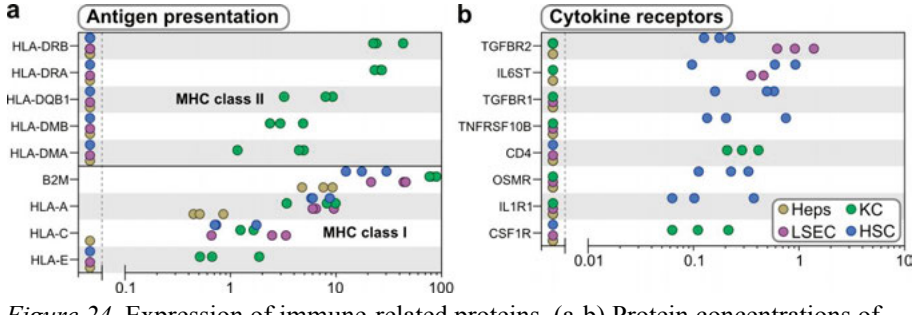

Figure 24. Expression of immune-related proteins. (a-b) Protein concentrations of (a) antigen presentation proteins and (b) cytokine receptors in the four different cell types.

However, some immune-related proteins, such as cytokine receptors, were predominantly expressed in other cell types (notably HSC; Figure 24b), and the proteomic data described here can thus provide informed starting points for more in-depth studies into the causes of idiosyncratic DILI.

Finally, the expression of SLC transporters, ABC transporters, and CYP enzymes was studied. Sixteen transporters of importance in drug development[67,74,75] were reliably quantified (by at least three unique peptides), out of which twelve were predominantly expressed in hepatocytes. The most highly expressed of the important SLC transporters were SLCO1B1, SLC22A1, SLCO1B3, and SLCO2B1 (Figure 25a), which is in line with proteomic results from intact liver tissue.[141,176] Interestingly, the SLCO transporters also showed some expression in KC. This matches previous observations on the expression of SLCO2B1 and SLCO4C1 (which was exclusive to KC here) in human blood macrophages.[177] In terms of ABC transporters, all but ABCC4 showed predominant expression in hepatocytes (Figure 25b). In fact, ABCC4 has previously been shown to be expressed by HSC,[178] which was the cell type with the highest levels of this transporter here.

Hepatocytes showed the highest expression of all CYP enzymes of importance in drug metabolism,[77] i.e. CYP3A4, CYP2D6, CYP2C9, CYP1A2, CYP2B6, CYP2C19, CYP2C8, CYP2A6, CYP2E1, and CYP2J2 (Figure 25c). Curiously, some CYPs were also present in KC, which might indicate an active role of these cells in drug metabolism. In general, however, the results supported the notion that hepatocytes perform the majority of ADME-related functions in the liver.

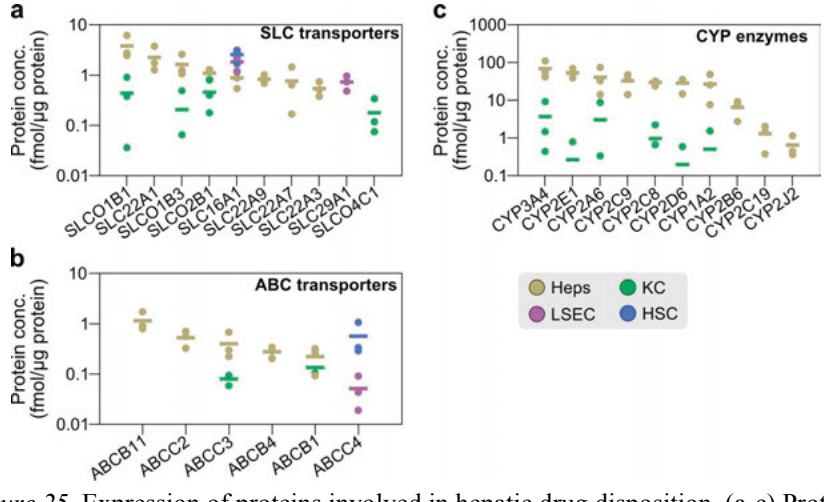

Figure 25. Expression of proteins involved in hepatic drug disposition. (a-c) Protein concentrations of (a) SLC transporters, (b) ABC transporters, and (c) CYP enzymes in the four different cell types. Missing data points indicate that the protein was not reliably quantified.

Conclusions

This thesis provides improved understanding and applicability of Caco-2 cells and primary human hepatocytes, two of the most important *in vitro* models for studies of small intestinal and hepatic drug disposition, respectively. Analysis of the Caco-2 proteome gave a description of its *in vivo*-likeness, and revealed aspects to consider for generating predictive transport data. While investigating human hepatocytes of different qualities, proteomics offered clues into the stress-related factors behind cryopreservation-induced non-attachment, which was used as a basis for ameliorating the problem. This work also led to a spin-off project in which a novel method for apoptosis detection was developed. Focus was then turned to liver zonation, where it was found that hepatocyte size reflects zonal origin, both in proteomic and functional terms. Finally, the proteomes of major NPC types were analyzed, providing a resource for exploring global and cell-type-specific expression patterns in the human liver.

From the work presented herein, it can be concluded that:

- The proteome of filter-grown Caco-2 cells contains many proteins related to enterocyte differentiation, as well as 112 SLC and 20 ABC transporters. Further, protein expression differences between Caco-2 and jejunum need to be considered for correctly interpreting transport studies *in vitro*.

- Apoptosis inhibition can be used to restore attachment properties and functionality of suboptimal hepatocyte batches after cryopreservation, without undesirable changes to the hepatocyte proteome.

- Quantification of cell debris in bright-field microscopy images can be used as a measure of late-stage apoptosis levels.

- Hepatocyte size corresponds to zonal origin, meaning that size separation of human hepatocytes can be used to study zone-specific functions in a way that cannot be done with whole-batch experiments.

- Human hepatocytes, LSEC, KC, and HSC all have unique proteomes, with contributions from the NPCs in some aspects of drug disposition.

Populärvetenskaplig sammanfattning

För att nå blodomloppet, och så småningom sitt tilltänkta mål, måste ett oralt administrerat läkemedel först absorberas genom tunntarmens slemhinna och sedan undvika alltför omfattande nedbrytning i levern. Att studera dessa parametrar är därför en viktig del av läkemedelsutvecklingsprocessen. Det kan åstadkommas i laboratoriemiljö genom användning av cellbaserade modeller som simulerar funktionen hos mänsklig tunntarm och lever, till exempel med Caco-2-celler och isolerade mänskliga hepatocyter. Ingen modell är dock optimal i alla lägen. Målet med denna avhandling var därför att öka förståelsen och tillämpbarheten för dessa cellmodeller, genom att kombinera moderna metoder för mätning av cellernas totala uttryck av proteiner (så kallad proteomik), de molekyler som utför cellens funktion, med olika slags funktionella studier.

I första skedet användes proteomik för detaljerad analys av Caco-2-celler, en mycket vanlig cellinje för att uppskatta läkemedelsabsorption i läkemedelsutveckling. Analysen lyfte fram på vilka sätt dessa celler liknade riktiga tarmceller, samt på vilka sätt de var mindre lika. Genom experimentella bestämningar av läkemedelsupptag och jämförelser med proteinuttryck i mänsklig tarmvävnad kunde också vikten av att ta hänsyn till skillnader mellan Caco-2-celler och tarmen belysas.

Fokus vändes sedan mot hepatocyter, de celler som huvudsakligen ansvarar för leverns funktion. Isolerade mänskliga hepatocyter används ofta i laboratorieexperiment för att studera läkemedelsupptag, metabolism och toxicitet i levern. Oftast har forskare dock bara tillgång till frysta celler, som ibland kraftigt skadas av den stress som orsakas av nedfrysnings- och upptiningsprocedurerna, vilket i värsta fall medför att cellerna inte går att använda. Här användes proteomik som en startpunkt för att utveckla ett stressreducerande protokoll för att lindra denna skada efter upptining, vilket tidigare inte ansetts möjligt. Detta enkla protokoll, som fungerar genom att hindra celldöd via så kallad apoptos, har potential att dramatiskt öka tillgången på högkvalitativa mänskliga hepatocyter. I samband med det här projektet utvecklades också en ny metod för att mäta apoptos, baserad på att räkna de partiklar celler ger ifrån sig när de dör på detta sätt.

Härnäst undersöktes de slående olikheter hepatocyter uppvisar på mikronivå i levern, så kallad leverzonering. Detta fenomen innebär att olika hepatocyter utför olika funktioner, beroende på deras placering i leverns finstruktur.

Det visade sig att isolerade hepatocytberedningar innehåller ett brett storleksspann av celler. Genom att dela upp hepatocyterna i olika storleksfraktioner och studera dem med proteomik och funktionella experiment framgick det att hepatocytstorlek i hög grad stämmer överens med cellens ursprungliga position i levervävnaden. Det betyder att storleksseparation kan användas som ett enkelt sätt att studera leverzonering i laboratoriemiljö.

Slutligen, eftersom hepatocyter inte är ensamma i levern, användes proteomik för att studera andra viktiga levercelltyper, så kallade icke-parenkymala celler. Här inkluderades de tre viktigaste icke-parenkymala celltyperna, det vill säga sinusoidala endotelceller, som bygger upp de finaste blodkärlen i levern, Kupfferceller, ett slags leverspecifika makrofager, samt stellatceller, som hjälper till att reglera blodflödet och lagrar vitamin A. Analysen visade att de olika celltyperna hade unika proteinuttrycksprofiler och tycktes alla på olika sätt bidra till leverns behandling av läkemedel. Datat från denna analys kan användas av forskningssamhället som en resurs för detaljerad utforskning av hur samspelet mellan olika slags leverceller reglerar och påverkar leverns funktion.

Sammanfattningsvis bidrar detta avhandlingsarbete till ökad förståelse och utökade tillämpningsmöjligheter för Caco-2-celler och mänskliga hepatocyter, två av de allra viktigaste laboratoriemodellerna för att studera hur tunntarmen och levern behandlar ett administrerat läkemedel.

Acknowledgements

The work presented in this thesis was carried out at the Department of Pharmacy, Faculty of Pharmacy, Uppsala University, Sweden. The studies were financially supported by the Swedish Research Council. IF:s stiftelse för farmacevtisk forskning, Elisabeth och Alfred Ahlqvists stiftelse, and Anna Maria Lundins stipendiefond are gratefully acknowledged for the travel grants that allowed me to participate in international scientific conferences.

I would like to express my gratitude to everyone who helped make this thesis a reality, and made my years in Uppsala so enjoyable.

First, my supervisors and co-supervisors:

Per Artursson, for giving me the freedom to pursue my own scientific ideas beyond the scope of initial outlines. Your style of supervision, while befuddling at first, has instilled in me an independence I would not have believed possible at the outset, for which I thank you. It has been a long, and sometimes winding, road, but I have come to realize that science is rarely a straight path from here to there.

Pär Matsson, for being a beacon of Norrlandish calm in any analytical weather. Even though the frequency of our interactions decreased as time went on, I am grateful for the analytical and stylistic guidance you have given me.

Ed LeCluyse, for your vast knowledge of everything hepatocyte-related, which was very helpful in the early stages of my thesis work. It was fun to set up the elutriator together. It has been my favorite piece of equipment ever since. Thank you, also, for letting me hang out in your lab for a week, and for showing me around Chapel Hill.

I want to thank all my co-authors, without whom the studies that constitute this thesis would not have been possible. Jacek Wiśniewski, for all your proteomic analyses, for hosting me in your lab for two weeks, and for sharing some Bavarian culture with me. Jozef Urdzik, for your skill and patience in our collaborative liver projects. Inken, my excellent master student, for all the cool data. It was great to be a part of your early steps in the world of science.

To my fellow PhD students in the drug delivery group:

André, getting to know you has been a wonderful and flabbergasting experience. It was like our minds somehow synchronized in the conjuring of nerdy

ideas, creating new levels of nerdiness incomprehensible to the outside world. Conversations were never the same after you left.

Andrea, your passion for classical music is an inspiration. I really appreciate our talks over the years. While normally quite calm, I also like when the sleeping Swiss patriot wakes up (perhaps at the mention of the height of Swedish mountains)…

Christine, I am truly grateful for our constant bouncing of ideas back and forth, as well as your listening ear whenever I needed to vent some frustration. This has been immensely helpful more times than I can count. Also, it was great fun writing the Gini paper together. By the way, who will know where anything is in the lab when you leave?

Niklas, it was nice to have another engineer join the group. I always enjoy digging into data together, even though stuff regularly flies over my head when you start talking mathematics…

Signe, our time together was a bit shorter, but it was so much fun to practice my fake Danish with you (while also learning some real words!). Good luck with all those cool graphs you keep making all the time.

Anna, thanks for setting in motion the proteomics-related aspects of our group, which became such an important (and interesting) part of my thesis.

Linda, I could not have wished for a more amazing office buddy. Thanks for the laughs, the Christmas decorations, and all the wisdom. To think that we both finished enough to-do lists to write a thesis… Spectacular!

Caroline, I never had as much fun teaching as when we were lab D buddies, or as much fun toasting as when we were toastmaster buddies! Thanks for helping me navigate the world of color, and for sharing my taste for pastel.

All other PhD students in the Kicki group, thanks for making the hallway and our common meetings interesting places to be.

Thanks to all members of the drug delivery group, past and present, for making our lab into such a dynamic and fun environment to work in. Special thanks to Elin for your excellent coordination of our hepatocyte activities, to Patrik for your massive knowledge of anything physiological, to Fabienne for our awesome trip to the US, to Ursula for being the sunniest person on the planet, to Tomás for weird but always enjoyable discussions, and to Janneke and Vicky for briefly sharing my office and for teaching me the strange ways of the Dutch and the Greek.

I would also like to thank all the other PhD students at the department for the great atmosphere we had during lunches, after works, PhD student days, meetings, and so on. Special thanks to Calle for all the good times, in and out of work, and for being almost the only one at work to share my interest for sports. I can barely see a football manager these days without thinking of you.

Huge thanks to my mom and dad for sparking my sense of curiosity and craving for knowledge from an early age, and for always supporting me in the choices I make.

Last, but definitely not least, huge thanks to my wonderful, marvelous little family. Annelie, you are the best thing that ever happened to me. Thank you for being you, and for taking me with you into the world of birds. Also, I am so grateful for your remarkable patience when I was writing this book. *Ja' älsk' du*. Ivar, you are the most amazing guy I know. Every day with you is an adventure.

References

1 Hidalgo, I. J., Raub, T. J. & Borchardt, R. T. Characterization of the human colon carcinoma cell line (Caco-2) as a model system for intestinal epithelial permeability. *Gastroenterology* **96**, 736-749 (1989).

2 Godoy, P. *et al.* Recent advances in 2D and 3D in vitro systems using primary hepatocytes, alternative hepatocyte sources and non-parenchymal liver cells and their use in investigating mechanisms of hepatotoxicity, cell signaling and ADME. *Arch Toxicol* **87**, 1315-1530 (2013).

3 Engle, M. J., Goetz, G. S. & Alpers, D. H. Caco-2 cells express a combination of colonocyte and enterocyte phenotypes. *J Cell Physiol* **174**, 362-369 (1998).

4 Rowe, C. *et al.* Proteome-wide analyses of human hepatocytes during differentiation and dedifferentiation. *Hepatology* **58**, 799-809 (2013).

5 Lauschke, V. M. *et al.* Massive rearrangements of cellular MicroRNA signatures are key drivers of hepatocyte dedifferentiation. *Hepatology* **64**, 1743-1756 (2016).

6 Elaut, G. *et al.* Molecular mechanisms underlying the dedifferentiation process of isolated hepatocytes and their cultures. *Curr Drug Metab* **7**, 629-660 (2006).

7 Shan, J. *et al.* Identification of small molecules for human hepatocyte expansion and iPS differentiation. *Nat Chem Biol* **9**, 514-520 (2013).

8 Ostrowska, A. *et al.* Investigation of functional and morphological integrity of freshly isolated and cryopreserved human hepatocytes. *Cell Tissue Bank* **1**, 55-68 (2000).

9 Alexandre, E. *et al.* Cryopreservation of adult human hepatocytes obtained from resected liver biopsies. *Cryobiology* **44**, 103-113 (2002).

10 Alexandre, E. *et al.* Plateable cryopreserved human hepatocytes for the assessment of cytochrome P450 inducibility: experimental condition-related variables affecting their response to inducers. *Xenobiotica* **42**, 968-979 (2012).

11 Baze, A. *et al.* Three-dimensional spheroid primary human hepatocytes in monoculture and coculture with nonparenchymal cells. *Tissue Eng Part C Methods* **24**, 534-545 (2018).

12 Gebhardt, R. & Matz-Soja, M. Liver zonation: novel aspects of its regulation and its impact on homeostasis. *World J Gastroenterol* **20**, 8491-8504 (2014).

13 Kmiec, Z. Cooperation of liver cells in health and disease. *Adv Anat Embryol Cell Biol* **161**, 1-151 (2001).

14 Aebersold, R. & Mann, M. Mass-spectrometric exploration of proteome structure and function. *Nature* **537**, 347-355 (2016).

15 Davis, S. S., Hardy, J. G. & Fara, J. W. Transit of pharmaceutical dosage forms through the small intestine. *Gut* **27**, 886-892 (1986).

16 Teitelbaum, E. N., Vaziri, K., Zettervall, S., Amdur, R. L. & Orkin, B. A. Intraoperative small bowel length measurements and analysis of demographic predictors of increased length. *Clin Anat* **26**, 827-832 (2013).

17 Boron, W. F. & Boulpaep, E. L. *Medical physiology* (Elsevier, 2017).

18 Madara, J. L. Functional morphology of epithelium of the small intestine, in *Handbook of Physiology: The Gastrointestinal System*, 83-120 (American Physiological Society, 1991).
19 van der Flier, L. G. & Clevers, H. Stem cells, self-renewal, and differentiation in the intestinal epithelium. *Annu Rev Physiol* **71**, 241-260 (2009).
20 Massey-Harroche, D. Epithelial cell polarity as reflected in enterocytes. *Microsc Res Tech* **49**, 353-362 (2000).
21 Moor, A. E. *et al.* Spatial reconstruction of single enterocytes uncovers broad zonation along the intestinal villus axis. *Cell* **175**, 1156-1167 (2018).
22 Blander, J. M. Death in the intestinal epithelium—basic biology and implications for inflammatory bowel disease. *FEBS J* **283**, 2720-2730 (2016).
23 Darwich, A. S., Aslam, U., Ashcroft, D. M. & Rostami-Hodjegan, A. Meta-analysis of the turnover of intestinal epithelia in preclinical animal species and humans. *Drug Metab Dispos* **42**, 2016-2022 (2014).
24 Helander, H. F. & Fändriks, L. Surface area of the digestive tract–revisited. *Scand J Gastroenterol* **49**, 681-689 (2014).
25 Bradley, S. E., Ingelfinger, F. J., Bradley, G. P. & Curry, J. J. The estimation of hepatic blood flow in man. *J Clin Invest* **24**, 890-897 (1945).
26 LeCluyse, E. L., Witek, R. P., Andersen, M. E. & Powers, M. J. Organotypic liver culture models: meeting current challenges in toxicity testing. *Crit Rev Toxicol* **42**, 501-548 (2012).
27 Gao, B., Jeong, W. I. & Tian, Z. Liver: An organ with predominant innate immunity. *Hepatology* **47**, 729-736 (2008).
28 Teutsch, H. F. The modular microarchitecture of human liver. *Hepatology* **42**, 317-325 (2005).
29 Hall, A. *et al.* Transaminase abnormalities and adaptations of the liver lobule manifest at specific cut-offs of steatosis. *Sci Rep* **7**, 40977 (2017).
30 Torre, C., Perret, C. & Colnot, S. Molecular determinants of liver zonation, in *Progress in Molecular Biology and Translational Science*, 127-150 (Elsevier, 2010).
31 Ben-Moshe, S. & Itzkovitz, S. Spatial heterogeneity in the mammalian liver. *Nat Rev Gastroenterol Hepatol* (2019).
32 Jungermann, K. & Kietzmann, T. Oxygen: modulator of metabolic zonation and disease of the liver. *Hepatology* **31**, 255-260 (2000).
33 Kietzmann, T. Metabolic zonation of the liver: the oxygen gradient revisited. *Redox Biol* **11**, 622-630 (2017).
34 Benhamouche, S. *et al.* Apc tumor suppressor gene is the "zonation-keeper" of mouse liver. *Dev Cell* **10**, 759-770 (2006).
35 Cheng, X. *et al.* Glucagon contributes to liver zonation. *Proc Natl Acad Sci U S A* **115**, E4111-E4119 (2018).
36 Brosch, M. *et al.* Epigenomic map of human liver reveals principles of zonated morphogenic and metabolic control. *Nat Commun* **9**, 4150 (2018).
37 Jungermann, K., Heilbronn, R., Katz, N. & Sasse, D. The glucose/glucose-6-phosphate cycle in the periportal and perivenous zone of rat liver. *Eur J Biochem* **123**, 429-436 (1982).
38 Häussinger, D. Hepatocyte heterogeneity in glutamine and ammonia metabolism and the role of an intercellular glutamine cycle during ureogenesis in perfused rat liver. *Eur J Biochem* **133**, 269-275 (1983).
39 Lindros, K. O. Zonation of cytochrome P450 expression, drug metabolism and toxicity in liver. *Gen Pharmacol Vasc S* **28**, 191-196 (1997).
40 Halpern, K. B. *et al.* Single-cell spatial reconstruction reveals global division of labour in the mammalian liver. *Nature* **542**, 352-356 (2017).

41 MacParland, S. A. *et al.* Single cell RNA sequencing of human liver reveals distinct intrahepatic macrophage populations. *Nat Commun* **9**, 4383 (2018).
42 Turner, R. *et al.* Human hepatic stem cell and maturational liver lineage biology. *Hepatology* **53**, 1035-1045 (2011).
43 Wang, M.-J., Chen, F., Lau, J. T. & Hu, Y.-P. Hepatocyte polyploidization and its association with pathophysiological processes. *Cell Death Dis* **8**, e2805 (2017).
44 Celton-Morizur, S. & Desdouets, C. Polyploidization of liver cells, in *Polyploidization and cancer*, 123-135 (Springer, 2010).
45 Uchiyama, Y. & Asari, A. A morphometric study of the variations in subcellular structures of rat hepatocytes during 24 hours. *Cell Tissue Res* **236**, 305-315 (1984).
46 Ferri, D. *et al.* Ultrastructural zonal heterogeneity of hepatocytes and mitochondria within the hepatic acinus during liver regeneration after partial hepatectomy. *Biol Cell* **97**, 277-288 (2005).
47 Wisse, E., Jacobs, F., Topal, B., Frederik, P. & De Geest, B. The size of endothelial fenestrae in human liver sinusoids: implications for hepatocyte-directed gene transfer. *Gene Ther* **15**, 1193-1199 (2008).
48 Horn, T., Christoffersen, P. & Henriksen, J. H. Alcoholic liver injury: defenestration in noncirrhotic livers—a scanning electron microscopic study. *Hepatology* **7**, 77-82 (1987).
49 Sørensen, K. K., Simon-Santamaria, J., McCuskey, R. S. & Smedsrød, B. Liver sinusoidal endothelial cells. *Compr Physiol* **5**, 1751-1774 (2011).
50 Bilzer, M., Roggel, F. & Gerbes, A. L. Role of Kupffer cells in host defense and liver disease. *Liver Int* **26**, 1175-1186 (2006).
51 Broadley, S. P. *et al.* Dual-track clearance of circulating bacteria balances rapid restoration of blood sterility with induction of adaptive immunity. *Cell Host Microbe* **20**, 36-48 (2016).
52 Zeng, Z. *et al.* CRIg functions as a macrophage pattern recognition receptor to directly bind and capture blood-borne gram-positive bacteria. *Cell Host Microbe* **20**, 99-106 (2016).
53 Kolios, G., Valatas, V. & Kouroumalis, E. Role of Kupffer cells in the pathogenesis of liver disease. *World J Gastroenterol* **12**, 7413-7420 (2006).
54 Roberts, R. A. *et al.* Role of the Kupffer cell in mediating hepatic toxicity and carcinogenesis. *Toxicol Sci* **96**, 2-15 (2006).
55 Rose, K. A., Holman, N. S., Green, A. M., Andersen, M. E. & LeCluyse, E. L. Co-culture of hepatocytes and Kupffer cells as an in vitro model of inflammation and drug-induced hepatotoxicity. *J Pharm Sci* **105**, 950-964 (2016).
56 Hellerbrand, C. Hepatic stellate cells—the pericytes in the liver. *Pflugers Arch* **465**, 775-778 (2013).
57 Zhang, C. Y., Yuan, W. G., He, P., Lei, J. H. & Wang, C. X. Liver fibrosis and hepatic stellate cells: etiology, pathological hallmarks and therapeutic targets. *World J Gastroenterol* **22**, 10512-10522 (2016).
58 Sugano, K. *et al.* Coexistence of passive and carrier-mediated processes in drug transport. *Nat Rev Drug Discov* **9**, 597-614 (2010).
59 Di, L. *et al.* Evidence-based approach to assess passive diffusion and carrier-mediated drug transport. *Drug Discov Today* **17**, 905-912 (2012).
60 Smith, D. *et al.* Passive lipoidal diffusion and carrier-mediated cell uptake are both important mechanisms of membrane permeation in drug disposition. *Mol Pharm* **11**, 1727-1738 (2014).

61 Lande, M. B., Donovan, J. M. & Zeidel, M. L. The relationship between membrane fluidity and permeabilities to water, solutes, ammonia, and protons. *J Gen Physiol* **106**, 67-84 (1995).
62 Assimakopoulos, S. F., Papageorgiou, I. & Charonis, A. Enterocytes' tight junctions: from molecules to diseases. *World J Gastrointest Pathophysiol* **2**, 123-137 (2011).
63 Turner, J. R., Buschmann, M. M., Romero-Calvo, I., Sailer, A. & Shen, L. The role of molecular remodeling in differential regulation of tight junction permeability. *Semin Cell Dev Biol* **36**, 204-212 (2014).
64 Tamura, A. & Tsukita, S. Paracellular barrier and channel functions of TJ claudins in organizing biological systems: advances in the field of barriology revealed in knockout mice. *Semin Cell Dev Biol* **36**, 177-185 (2014).
65 Adson, A. *et al.* Passive diffusion of weak organic electrolytes across Caco-2 cell monolayers: Uncoupling the contributions of hydrodynamic, transcellular, and paracellular barriers. *J Pharm Sci* **84**, 1197-1204 (1995).
66 Flanagan, S. D., Takahashi, L. H., Liu, X. & Benet, L. Z. Contributions of saturable active secretion, passive transcellular, and paracellular diffusion to the overall transport of furosemide across adenocarcinoma (Caco-2) cells. *J Pharm Sci* **91**, 1169-1177 (2002).
67 Giacomini, K. M. *et al.* Membrane transporters in drug development. *Nat Rev Drug Discov* **9**, 215-236 (2010).
68 Mateus, A. *et al.* Intracellular drug bioavailability: a new predictor of system dependent drug disposition. *Sci Rep* **7**, 43047 (2017).
69 Lin, L., Yee, S. W., Kim, R. B. & Giacomini, K. M. SLC transporters as therapeutic targets: emerging opportunities. *Nat Rev Drug Discov* **14**, 543-560 (2015).
70 Vasiliou, V., Vasiliou, K. & Nebert, D. W. Human ATP-binding cassette (ABC) transporter family. *Hum Genomics* **3**, 281-290 (2009).
71 O'Hagan, S., Muelas, M. W., Day, P. J., Lundberg, E. & Kell, D. B. GeneGini: assessment via the Gini coefficient of reference "housekeeping" genes and diverse human transporter expression profiles. *Cell Syst* **6**, 230-244 (2018).
72 Nigam, S. K. What do drug transporters really do? *Nat Rev Drug Discov* **14**, 29-44 (2015).
73 Zamek-Gliszczynski, M. J. *et al.* ITC recommendations for transporter kinetic parameter estimation and translational modeling of transport-mediated PK and DDIs in humans. *Clin Pharmacol Ther* **94**, 64-79 (2013).
74 Hillgren, K. M. *et al.* Emerging transporters of clinical importance: an update from the International Transporter Consortium. *Clin Pharmacol Ther* **94**, 52-63 (2013).
75 Zamek-Gliszczynski, M. J. *et al.* Transporters in drug development: 2018 ITC recommendations for transporters of emerging clinical importance. *Clin Pharmacol Ther* **104**, 890-899 (2018).
76 Sheweita, S. A. Drug-metabolizing enzymes mechanisms and functions. *Curr Drug Metab* **1**, 107-132 (2000).
77 Zanger, U. M. & Schwab, M. Cytochrome P450 enzymes in drug metabolism: regulation of gene expression, enzyme activities, and impact of genetic variation. *Pharmacol Ther* **138**, 103-141 (2013).
78 Jancova, P., Anzenbacher, P. & Anzenbacherova, E. Phase II drug metabolizing enzymes. *Biomed Pap Med Fac Univ Palacky Olomouc Czech Repub* **154**, 103-116 (2010).
79 Bleibel, W., Kim, S., D'Silva, K. & Lemmer, E. R. Drug-induced liver injury. *Dig Dis Sci* **52**, 2463-2471 (2007).

80 Lee, W. M. Drug-induced hepatotoxicity. *N Engl J Med* **349**, 474-485 (2003).
81 Kullak-Ublick, G. A. *et al.* Drug-induced liver injury: recent advances in diagnosis and risk assessment. *Gut* **66**, 1154-1164 (2017).
82 Mosedale, M. & Watkins, P. B. Drug-induced liver injury: advances in mechanistic understanding that will inform risk management. *Clin Pharmacol Ther* **101**, 469-480 (2017).
83 Aleo, M. D. *et al.* Human drug-induced liver injury severity is highly associated with dual inhibition of liver mitochondrial function and bile salt export pump. *Hepatology* **60**, 1015-1022 (2014).
84 Iorga, A., Dara, L. & Kaplowitz, N. Drug-induced liver injury: cascade of events leading to cell death, apoptosis or necrosis. *Int J Mol Sci* **18**, 1018 (2017).
85 Deferme, S., Annaert, P. & Augustijns, P. In vitro screening models to assess intestinal drug absorption and metabolism, in *Drug absorption studies*, 182-215 (Springer, 2008).
86 Zeilinger, K., Freyer, N., Damm, G., Seehofer, D. & Knöspel, F. Cell sources for in vitro human liver cell culture models. *Exp Biol Med* **241**, 1684-1698 (2016).
87 Kansy, M., Senner, F. & Gubernator, K. Physicochemical high throughput screening: parallel artificial membrane permeation assay in the description of passive absorption processes. *J Med Chem* **41**, 1007-1010 (1998).
88 Sugano, K., Hamada, H., Machida, M. & Ushio, H. High throughput prediction of oral absorption: improvement of the composition of the lipid solution used in parallel artificial membrane permeation assay. *J Biomol Screen* **6**, 189-196 (2001).
89 Fogh, J., Wright, W. C. & Loveless, J. D. Absence of HeLa cell contamination in 169 cell lines derived from human tumors. *J Natl Cancer Inst* **58**, 209-214 (1977).
90 Grasset, E., Pinto, M., Dussaulx, E., Zweibaum, A. & Desjeux, J. F. Epithelial properties of human colonic carcinoma cell line Caco-2: electrical parameters. *Am J Physiol Cell Physiol* **247**, C260-C267 (1984).
91 Pinto, M. *et al.* Enterocyte-like differentiation and polarization of the human colon carcinoma cell line Caco-2 in culture. *Biol Cell* **47**, 323-330 (1983).
92 Artursson, P., Palm, K. & Luthman, K. Caco-2 monolayers in experimental and theoretical predictions of drug transport. *Adv Drug Deliv Rev* **22**, 67-84 (1996).
93 Hubatsch, I., Ragnarsson, E. G. E. & Artursson, P. Determination of drug permeability and prediction of drug absorption in Caco-2 monolayers. *Nat Protoc* **2**, 2111-2119 (2007).
94 Linnankoski, J. *et al.* Paracellular porosity and pore size of the human intestinal epithelium in tissue and cell culture models. *J Pharm Sci* **99**, 2166-2175 (2010).
95 Ben-David, U. *et al.* Genetic and transcriptional evolution alters cancer cell line drug response. *Nature* **560**, 325-330 (2018).
96 Hughes, P., Marshall, D., Reid, Y., Parkes, H. & Gelber, C. The costs of using unauthenticated, over-passaged cell lines: how much more data do we need? *Biotechniques* **43**, 575-586 (2007).
97 Hayeshi, R. *et al.* Comparison of drug transporter gene expression and functionality in Caco-2 cells from 10 different laboratories. *Eur J Pharm Sci* **35**, 383-396 (2008).

98 Kuteykin-Teplyakov, K., Luna-Tortos, C., Ambroziak, K. & Loscher, W. Differences in the expression of endogenous efflux transporters in MDR1-transfected versus wildtype cell lines affect P-glycoprotein mediated drug transport. *Br J Pharmacol* **160**, 1453-1463 (2010).
99 Grass, G. M. & Sweetana, S. A. In vitro measurement of gastrointestinal tissue permeability using a new diffusion cell. *Pharm Res* **5**, 372-376 (1988).
100 Sison-Young, R. L. *et al.* A multicenter assessment of single-cell models aligned to standard measures of cell health for prediction of acute hepatotoxicity. *Arch Toxicol* **91**, 1385-1400 (2017).
101 Gerets, H. H. *et al.* Characterization of primary human hepatocytes, HepG2 cells, and HepaRG cells at the mRNA level and CYP activity in response to inducers and their predictivity for the detection of human hepatotoxins. *Cell Biol Toxicol* **28**, 69-87 (2012).
102 Bell, C. C. *et al.* Transcriptional, functional, and mechanistic comparisons of stem cell-derived hepatocytes, HepaRG cells, and three-dimensional human hepatocyte spheroids as predictive in vitro systems for drug-induced liver injury. *Drug Metab Dispos* **45**, 419-429 (2017).
103 LeCluyse, E. L. & Alexandre, E. Isolation and culture of primary hepatocytes from resected human liver tissue, in *Hepatocytes. Methods in Molecular Biology (Methods and Protocols)*, 57-82 (Humana Press, 2010).
104 Lee, S. M. *et al.* An algorithm that predicts the viability and the yield of human hepatocytes isolated from remnant liver pieces obtained from liver resections. *PLoS One* **9**, e107567 (2014).
105 Vondran, F. W. R. *et al.* Isolation of primary human hepatocytes after partial hepatectomy: criteria for identification of the most promising liver specimen. *Artif Organs* **32**, 205-213 (2008).
106 Lee, S. M., Schelcher, C., Demmel, M., Hauner, M. & Thasler, W. E. Isolation of human hepatocytes by a two-step collagenase perfusion procedure. *J Vis Exp* **79** (2013).
107 Hewitt, N. J. Optimisation of the cryopreservation of primary hepatocytes. *Methods Mol Biol* **640**, 83-105 (2010).
108 Stéphenne, X., Najimi, M. & Sokal, E. M. Hepatocyte cryopreservation: is it time to change the strategy? *World J Gastroenterol* **16**, 1-14 (2010).
109 Hewitt, N. J. & Li, A. P. Cryopreservation of hepatocytes, in *Protocols in In Vitro Hepatocyte Research*, 13-26 (Springer, 2015).
110 Khetani, S. R. *et al.* Microengineered liver tissues for drug testing. *J Lab Autom* **20**, 216-250 (2015).
111 Zvibel, I., Smets, F. & Soriano, H. Anoikis: roadblock to cell transplantation? *Cell Transplant* **11**, 621-630 (2002).
112 Smets, F. N., Chen, Y., Wang, L.-J. & Soriano, H. E. Loss of cell anchorage triggers apoptosis (anoikis) in primary mouse hepatocytes. *Mol Genet Metab* **75**, 344-352 (2002).
113 Soldatow, V. Y., Lecluyse, E. L., Griffith, L. G. & Rusyn, I. In vitro models for liver toxicity testing. *Toxicol Res* **2**, 23-39 (2013).
114 Smith, C. M. *et al.* A comprehensive evaluation of metabolic activity and intrinsic clearance in suspensions and monolayer cultures of cryopreserved primary human hepatocytes. *J Pharm Sci* **101**, 3989-4002 (2012).
115 Dunn, J. C., Tompkins, R. G. & Yarmush, M. L. Long-term in vitro function of adult hepatocytes in a collagen sandwich configuration. *Biotechnol Prog* **7**, 237-245 (1991).

116 LeCluyse, E. L., Audus, K. L. & Hochman, J. H. Formation of extensive canalicular networks by rat hepatocytes cultured in collagen-sandwich configuration. *Am J Physiol* **266**, C1764-1774 (1994).
117 Swift, B., Pfeifer, N. D. & Brouwer, K. L. Sandwich-cultured hepatocytes: an in vitro model to evaluate hepatobiliary transporter-based drug interactions and hepatotoxicity. *Drug Metab Rev* **42**, 446-471 (2010).
118 Pedersen, J. M. *et al.* Early identification of clinically relevant drug interactions with the human bile salt export pump (BSEP/ABCB11). *Toxicol Sci* **136**, 328-343 (2013).
119 Lauschke, V. M., Shafagh, R. Z., Hendriks, D. F. G. & Ingelman-Sundberg, M. 3D primary hepatocyte culture systems for analyses of liver diseases, drug metabolism and toxicity: Emerging culture paradigms and applications. *Biotechnol J*, e1800347 (2019).
120 Landry, J., Bernier, D., Ouellet, C., Goyette, R. & Marceau, N. Spheroidal aggregate culture of rat liver cells: histotypic reorganization, biomatrix deposition, and maintenance of functional activities. *J Cell Biol* **101**, 914-923 (1985).
121 Bell, C. C. *et al.* Characterization of primary human hepatocyte spheroids as a model system for drug-induced liver injury, liver function and disease. *Sci Rep* **6**, 25187 (2016).
122 Vorrink, S. U. *et al.* Endogenous and xenobiotic metabolic stability of primary human hepatocytes in long-term 3D spheroid cultures revealed by a combination of targeted and untargeted metabolomics. *Faseb j* **31**, 2696-2708 (2017).
123 Messner, S., Agarkova, I., Moritz, W. & Kelm, J. M. Multi-cell type human liver microtissues for hepatotoxicity testing. *Arch Toxicol* **87**, 209-213 (2013).
124 Bell, C. C. *et al.* Comparison of hepatic 2D sandwich cultures and 3D spheroids for long-term toxicity applications: a multicenter study. *Toxicol Sci* **162**, 655-666 (2018).
125 Knowles, B. B., Howe, C. C. & Aden, D. P. Human hepatocellular carcinoma cell lines secrete the major plasma proteins and hepatitis B surface antigen. *Science* **209**, 497-499 (1980).
126 Gripon, P. *et al.* Infection of a human hepatoma cell line by hepatitis B virus. *Proc Natl Acad Sci U S A* **99**, 15655-15660 (2002).
127 Vogel, C. & Marcotte, E. M. Insights into the regulation of protein abundance from proteomic and transcriptomic analyses. *Nat Rev Genet* **13**, 227-232 (2012).
128 Edfors, F. *et al.* Gene-specific correlation of RNA and protein levels in human cells and tissues. *Mol Syst Biol* **12**, 883 (2016).
129 Nagaraj, N. *et al.* Deep proteome and transcriptome mapping of a human cancer cell line. *Mol Syst Biol* **7**, 548 (2011).
130 Lewis, P. A. *et al.* Genome, transcriptome and proteome: the rise of omics data and their integration in biomedical sciences. *Brief Bioinform* **19**, 286-302 (2016).
131 Gillet, L. C., Leitner, A. & Aebersold, R. Mass spectrometry applied to bottom-up proteomics: entering the high-throughput era for hypothesis testing. *Annu Rev Anal Chem* **9**, 449-472 (2016).
132 Domon, B. & Aebersold, R. Options and considerations when selecting a quantitative proteomics strategy. *Nat Biotechnol* **28**, 710-721 (2010).
133 Wegler, C. *et al.* Variability in mass spectrometry-based quantification of clinically relevant drug transporters and drug metabolizing enzymes. *Mol Pharm* **14**, 3142-3151 (2017).
134 Kim, M.-S. *et al.* A draft map of the human proteome. *Nature* **509**, 575-581 (2014).

135 Wilhelm, M. *et al.* Mass-spectrometry-based draft of the human proteome. *Nature* **509**, 582-587 (2014).
136 Wang, D. *et al.* A deep proteome and transcriptome abundance atlas of 29 healthy human tissues. *Mol Syst Biol* **15**, e8503 (2019).
137 Claydon, A. J. & Beynon, R. Proteome dynamics: revisiting turnover with a global perspective. *Mol Cell Proteomics* **11**, 1551-1565 (2012).
138 Boisvert, F. M. *et al.* A quantitative spatial proteomics analysis of proteome turnover in human cells. *Mol Cell Proteomics* **11**, M111.011429 (2012).
139 Mathieson, T. *et al.* Systematic analysis of protein turnover in primary cells. *Nat Commun* **9**, 689 (2018).
140 Harper, J. W. & Bennett, E. J. Proteome complexity and the forces that drive proteome imbalance. *Nature* **537**, 328-338 (2016).
141 Vildhede, A., Wiśniewski, J. R., Norén, A., Karlgren, M. & Artursson, P. Comparative proteomic analysis of human liver tissue and isolated hepatocytes with a focus on proteins determining drug exposure. *J Proteome Res* **14**, 3305-3314 (2015).
142 Urdzik, J. *et al.* Global proteome changes in liver tissue 6 weeks after FOLFOX treatment of colorectal cancer liver metastases. *Proteomes* **4** (2016).
143 Horgan, R. P. & Kenny, L. C. 'Omic' technologies: genomics, transcriptomics, proteomics and metabolomics. *Obstet Gynaecol* **13**, 189-195 (2011).
144 Khatri, P., Sirota, M. & Butte, A. J. Ten years of pathway analysis: current approaches and outstanding challenges. *PLoS Comput Biol* **8**, e1002375 (2012).
145 Kanehisa, M. & Goto, S. KEGG: kyoto encyclopedia of genes and genomes. *Nucleic Acids Res* **28**, 27-30 (2000).
146 Fabregat, A. *et al.* The Reactome Pathway Knowledgebase. *Nucleic Acids Res* **46**, D649-D655 (2018).
147 Muruganujan, A., Ebert, D., Mi, H., Thomas, P. D. & Huang, X. PANTHER version 14: more genomes, a new PANTHER GO-slim and improvements in enrichment analysis tools. *Nucleic Acids Res* **47**, D419-D426 (2018).
148 Huang, D. W., Sherman, B. T. & Lempicki, R. A. Bioinformatics enrichment tools: paths toward the comprehensive functional analysis of large gene lists. *Nucleic Acids Res* **37**, 1-13 (2008).
149 Wiśniewski, J. R. & Mann, M. Consecutive proteolytic digestion in an enzyme reactor increases depth of proteomic and phosphoproteomic analysis. *Anal Chem* **84**, 2631-2637 (2012).
150 Wiśniewski, J. R. & Gaugaz, F. Z. Fast and sensitive total protein and peptide assays for proteomic analysis. *Anal Chem* **87**, 4110-4116 (2015).
151 Cox, J. & Mann, M. MaxQuant enables high peptide identification rates, individualized ppb-range mass accuracies and proteome-wide protein quantification. *Nat Biotechnol* **26**, 1367-1372 (2008).
152 Wiśniewski, J. R. & Rakus, D. Multi-enzyme digestion FASP and the 'Total Protein Approach'-based absolute quantification of the Escherichia coli proteome. *J Proteomics* **109**, 322-331 (2014).
153 Wiśniewski, J. R., Hein, M. Y., Cox, J. & Mann, M. A "proteomic ruler" for protein copy number and concentration estimation without spike-in standards. *Mol Cell Proteomics* **13**, 3497-3506 (2014).
154 Tyanova, S. *et al.* The Perseus computational platform for comprehensive analysis of (prote)omics data. *Nat Methods* **13**, 731-740 (2016).
155 Kramer, A., Green, J., Pollard, J., Jr. & Tugendreich, S. Causal analysis approaches in Ingenuity Pathway Analysis. *Bioinformatics* **30**, 523-530 (2014).

156 Bauer, S., Grossmann, S., Vingron, M. & Robinson, P. N. Ontologizer 2.0--a multifunctional tool for GO term enrichment analysis and data exploration. *Bioinformatics* **24**, 1650-1651 (2008).
157 Huang, D. W., Sherman, B. T. & Lempicki, R. A. Systematic and integrative analysis of large gene lists using DAVID bioinformatics resources. *Nat Protoc* **4**, 44-57 (2009).
158 Pathan, M. *et al.* FunRich: an open access standalone functional enrichment and interaction network analysis tool. *Proteomics* **15**, 2597-2601 (2015).
159 Vildhede, A. *et al.* Hepatic uptake of atorvastatin: influence of variability in transporter expression on uptake clearance and drug-drug interactions. *Drug Metab Dispos* **42**, 1210-1218 (2014).
160 Lennernäs, H. *et al.* Regional jejunal perfusion, a new in vivo approach to study oral drug absorption in man. *Pharm Res* **9**, 1243-1251 (1992).
161 Obach, R. S. Prediction of human clearance of twenty-nine drugs from hepatic microsomal intrinsic clearance data: An examination of in vitro half-life approach and nonspecific binding to microsomes. *Drug Metab Dispos* **27**, 1350-1359 (1999).
162 Cai, H., Dikalov, S., Griendling, K. K. & Harrison, D. G. Detection of reactive oxygen species and nitric oxide in vascular cells and tissues, in *Vascular Biology Protocols*, 293-311 (Humana Press, 2007).
163 Chan, L. L. *et al.* A rapid detection method for apoptosis and necrosis measurement using the Cellometer imaging cytometry. *Apoptosis* **16**, 1295-1303 (2011).
164 Wiśniewski, J. R. *et al.* Extensive quantitative remodeling of the proteome between normal colon tissue and adenocarcinoma. *Mol Syst Biol* **8**, 611 (2012).
165 Wiśniewski, J. R. *et al.* Absolute proteome analysis of colorectal mucosa, adenoma, and cancer reveals drastic changes in fatty acid metabolism and plasma membrane transporters. *J Proteome Res* **14**, 4005-4018 (2015).
166 Atkin-Smith, G. K. & Poon, I. K. Disassembly of the dying: mechanisms and functions. *Trends Cell Biol* **27**, 151-162 (2017).
167 Nagata, S., Hanayama, R. & Kawane, K. Autoimmunity and the clearance of dead cells. *Cell* **140**, 619-630 (2010).
168 Frisch, S. M. & Francis, H. Disruption of epithelial cell-matrix interactions induces apoptosis. *J Cell Biol* **124**, 619-626 (1994).
169 Pfaller, W. & Gstraunthaler, G. Nephrotoxicity testing in vitro--what we know and what we need to know. *Environ Health Perspect* **106**, 559-569 (1998).
170 Uhlén, M. *et al.* Tissue-based map of the human proteome. *Science* **347**, 1260419 (2015).
171 Ghafoory, S. *et al.* Zonation of nitrogen and glucose metabolism gene expression upon acute liver damage in mouse. *PLoS One* **8**, e78262 (2013).
172 Azimifar, S. B., Nagaraj, N., Cox, J. & Mann, M. Cell-type-resolved quantitative proteomics of murine liver. *Cell Metab* **20**, 1076-1087 (2014).
173 Ding, C. *et al.* A cell-type-resolved liver proteome. *Mol Cell Proteomics* **15**, 3190-3202 (2016).
174 Shanks, N., Greek, R. & Greek, J. Are animal models predictive for humans? *Philos Ethics Humanit Med* **4** (2009).
175 Seok, J. *et al.* Genomic responses in mouse models poorly mimic human inflammatory diseases. *Proc Natl Acad Sci U S A* **110**, 3507-3512 (2013).
176 Wiśniewski, J. R., Vildhede, A., Norén, A. & Artursson, P. In-depth quantitative analysis and comparison of the human hepatocyte and hepatoma cell line HepG2 proteomes. *J Proteomics* **136**, 234-247 (2016).

177 Moreau, A., Le Vee, M., Jouan, E., Parmentier, Y. & Fardel, O. Drug transporter expression in human macrophages. *Fundam Clin Pharmacol* **25**, 743-752 (2011).
178 Hannivoort, R. A. *et al.* Multidrug resistance–associated proteins are crucial for the viability of activated rat hepatic stellate cells. *Hepatology* **48**, 624-634 (2008).

Acta Universitatis Upsaliensis

Digital Comprehensive Summaries of Uppsala Dissertations from the Faculty of Pharmacy 272

Editor: The Dean of the Faculty of Pharmacy

A doctoral dissertation from the Faculty of Pharmacy, Uppsala University, is usually a summary of a number of papers. A few copies of the complete dissertation are kept at major Swedish research libraries, while the summary alone is distributed internationally through the series Digital Comprehensive Summaries of Uppsala Dissertations from the Faculty of Pharmacy. (Prior to January, 2005, the series was published under the title "Comprehensive Summaries of Uppsala Dissertations from the Faculty of Pharmacy".)

Distribution: publications.uu.se
urn:nbn:se:uu:diva-382406

ACTA
UNIVERSITATIS
UPSALIENSIS
UPPSALA
2019